GARTEUR GROUP FOR AERONAUTICAL RESEARCH AND TECHNOLOGY IN EUROPE

ORIGINAL: ENGLISH GARTEUR/TP-088-20

April 4, 1997

GARTEUR Open

RCAM Design Challenge Presentation Document: The Model Based Predictive Control Approach

by

Mihai Huzmezan
Jan Maciejowski

GROUP FOR AERONAUTICAL RESEARCH AND TECHNOLOGY IN EUROPE

ORIGINAL: ENGLISH GARTEUR/TP-088-20

April 4, 1997

GARTEUR Open

RCAM Design Challenge Presentation Document: The Model Based Predictive Control Approach

by

Mihai Huzmezan
Jan Maciejowski

This report has been prepared under auspices of the Responsables for Flight Mechanics, Systems and Integration of the Group for Aeronautical Research and Technology in EURope (GARTEUR)

Group of Resp.	:	FM-GoR	Action Group	:	FM(AG08)
Report Resp.	:	Jan Maciejowski/	Version	:	1
Project Man.	:	J.C. Terlouw/	Completed	:	September 25, 1997
Monitoring Resp.	:	J.T.M. van Doorn/			

List of authors

Mihai Huzmezan[1],
Jan Maciejowski[2]

1

University of Cambridge
Department of Engineering
Division F, Control Group
CB2 1PZ, Cambridge, U.K.
tel.+44-1223-339222, fax.+44-1223-332662
e-mail: mh2@eng.cam.ac.uk

2

University of Cambridge
Department of Engineering
Division F, Control Group
CB2 1PZ, Cambridge, U.K.
tel.+44-1223-332732, fax.+44-1223-332662
e-mail: jmm@eng.cam.ac.uk

Summary

This report applies Model Based Predictive Control (MBPC) to the Garteur RCAM Design Challenge. Separate controllers are proposed for the longitudinal and lateral channels, each of these having MBPC in the inner loop and a conventional controller in the outer loop. Emphasis is placed on describing the design process.

MBPC is not recommended for routine use in flight control, but has good potential for higher level control functions such as: on-board flight management and reconfiguration of controllers in event of damage and to the aircraft structure or equipment.

FM(AG08) Principal Persons

Ahmed S (UK)	CCL	1 copy
Ambrosino G (IT)	UNAP	1 copy
Bernussou J (FR)	LAAS	1 copy
Cruz J de la (ES)	UCM	1 copy
Delgado I (ES)	INTA	1 copy
Dormido S (ES)	UNED	1 copy
Duda H (DE)	DLR	1 copy
Escande B (FR)	ONERA	1 copy
Faleiro L (UK)	LUT	1 copy
Fielding C (UK)	BAe-MA	1 copy
Game G (UK)	BAeDD	1 copy
Gautrey J (UK)	CUN	1 copy
Helmersson A (SE)	LiTH	1 copy
Joos H (DE)	DLR	1 copy
Laidlaw D (UK)	AVRO	1 copy
Luckner R (DE)	DASA	1 copy
Maciejowski J (UK)	UCAM	1 copy
Magni J (FR)	ONERA	1 copy
Muir E (UK)	DRA	1 copy
Postlethwaite I (UK)	ULES	1 copy
Schram G (NL)	DUT-EE	1 copy
Ståhl-Gunnarsson K (SE)	SMA	1 copy
Terlouw J (NL)	NLR	1 copy
Tonon A (IT)	ALN	1 copy
Vaart J van der (NL)	DUT-AE	1 copy
Verde L (IT)	CIRA	1 copy

Members of the Flight Mechanics, Systems and Integration Group of Responsables

Brännström B (SE)	FMV	1 copy
Doorn J van (NL)	NLR	1 copy
England P (UK)	DRA	1 copy
Muñoz F (IT)	INTA	1 copy
Rodloff R (DE)	DLR	1 copy
Verbrugge R (FR)	ONERA	1 copy

Members of the Executive Committee

Chéret J (FR)	ONERA	1 copy
Coleman G (UK)	DRA	1 copy
Gustafsson A (SE)	FFA	1 copy
Haupt R (DE)	DLR/PD-L	1 copy
Moreno Labata G (ES)	INTA	1 copy
Slooff J (NL)	NLR	1 copy

Secretary GARTEUR

Jonasson K (SE)	FFA	1 copy

Contents

List of figures

List of tables

List of symbols and abbreviations

Symbols

The used symbols are in accordance with the nomenclature defined in the Communication Handbook [1].

Abbreviations

ALN	Alenia Aeronautica
ANDECS	ANalysis and DEsign of Controlled Systems
AS	Aérospatiale
AVRO	AVRO International Aerospace
BAeDD	British Aerospace Dynamics Division
BAe-MAD	British Aerospace Military Aircraft Division
CCL	Cambridge Control Ltd
CERT	Centre d'Etudes et de Recherces de Toulouse
CIRA	Centro Italiano Ricerche Aerospaziali S.p.A.
CUN	Cranfield University
DASA	Daimler-Benz Aerospace Airbus
DE	Germany
DLR	Deutsche Forschungsanstalt für Luft- und Raumfahrt (German Aerospace Research Establishment)
DRA	Defence Research Agency
DUT	Delft University of Technology
ES	Spain
FAC	Fokker Aircraft B.V.
FFA	Flygtekniska Försöksanstalten (The Aeronautical Research Institute of Sweden)
FMAG	Flight Mechanics Action Group
FM-GoR	Flight Mechanics, Systems and Integration Group of Responsables
FMV-F-FL	Försvarets Materielverk (Defense Material Administration)
FR	France
GARTEUR	Group for Aeronautical Research and Technology in EURope
GUN	Glasgow University
INTA	Instituto Nacional de Técnica Aerospacial (National Institute for Aerospace Technology)
IT	Italy
LiTH	Linköping University

LUT	Loughborough University of Technology
NIVR	Nederlands Instituut voor Vliegtuigontwikkeling en Ruimtevaart (Netherlands Agency for Aerospace Programs)
NL	the Netherlands
NLR	Nationaal Lucht- en Ruimtevaartlaboratorium (National Aerospace Laboratory, The Netherlands)
ONERA	Office National d'Etudes et de Recherches Aérospatiales (National Institute for Aerospace Research and Studies)
SE	Sweden
SMA	Saab Scania AB, Military Aircraft
UCAM	University of Cambridge
UK	United Kingdom
ULES	University of Leicester
UNAP	Universitá di Napoli "Fedirico II"
UNED	Universidad Nacional de Educación a Distancia
DMC	Dynamic Matrix Control
IDCOM	IDentification and COMmand
MBPC	Model Based Predictive Control
SAS	Stability Augmentation System

1 Introduction

The use of Model Based Predictive Control (MBPC) is increasing rapidly in the process industries, where it has proved to be extremely effective. MBPC is generally thought to be unsuitable for aerospace applications, because it involves on-line constrained optimisation, and is therefore likely to be too slow to deal with the relatively fast dynamics of aircraft, as well as presenting problems for certification. But this view does not take sufficient account of the astonishing speed of currently-available computers, or of the considerable increase in power still potentially available from CMOS technology.

We believe that MBPC may be useful in the realm of flight control — if not for "routine" use in closing conventional control loops, then perhaps for more exotic applications like reconfigurable control, or for on-board flight management systems. We were therefore motivated to take part in the GARTEUR flight control Design Challenge, to see how well MBPC could do even in a 'routine' application, and to acquire experience of MBPC design in the context of flight control.

MBPC has some very appealing attributes: *Simplicity* — the basic idea of MBPC is fairly intuitive, and can be understood without advanced mathematics; *Richness* — the common elements of MBPC schemes, such as models, objective functions, prediction horizons, etc, can be tailored to specific problems; and *Practicality* — the usual combination of linear dynamics and inequality constraints allows realistic nonlinearities to be handled without sacrificing too much speed. In process control it has become usual to represent the controlled plant by an input-output model when using MBPC. In this report we use a state-space model instead. This seems more natural for flight control, since the states can be chosen to be physical variables, and this correspondence can be exploited to some extent.

Most of the detailed work for this Report was done by M.Huzmezan, who has some background experience of flight control systems. Despite this, obtaining a satisfactory design required a lot of time-consuming iteration. In the course of this work we have produced a simulation framework which can be used for general MBPC applications, and this has reduced the "cycle time" of each design iteration considerably. We have also noticed that the amount of iteration reduces significantly as the designer's experience grows. One practical problem encountered was with the use of *Simulink*: the "mixed-mode" simulation required because of a continuous-time model and a discrete-time controller resulted in extremely low simulation speeds, which reduced the amount of design iteration that was feasible.

Acknowledgements

We would like to acknowledge Pembroke College Cambridge, Lundgren Fund, ORS scholarship, Cambridge Overseas Trust and CT Taylor Fund by which Mihai Huzmezan is supported.

2 A tutorial review of the applied control design methodology

2.1 Introduction

The design approach mainly adopted here is based on Model Based Predictive Control Techniques. Practical Model Based Predictive Control was discovered in the early 80's by development of heuristic, rather than theoretical algorithms such as IDCOM (Identification and Command) by Richalet [11] and by Cutler [6] in DMC (Dynamic Matrix Control). Another approach not entirely different is GPC (Generalised Predictive Control) due to Clarke [7]. In the period 1990-94 there has been significant progress in understanding of the design and use of MBPC control. MPBC nowadays enables the addition of actuator input or rate of change constraints as well of state constraints for which new stability theories are emerging. System properties like difficult dynamic behaviour, multivariable interactive systems, constraints are handled by MBPC.
The defining feature of MPBC is the repeated optimisation of a performance objective over a finite horizon extending from the current or some future time up to a prediction horizon. The main steps in applying MBPC are: the identification of the process model and tuning the design parameters. The optimisation uses an explicit plant model.
The basic principle of MBPC is accessible and many experiments and implementations have demonstrated that this technique is not difficult to use and it has a good performance/cost ratio. MBPC offer a wide range of choice in model structure, prediction methods and optimisation criteria. In recent years it has been realized that many control methods, which were successfully applied to real processes have in fact much in common, being variations of the MBPC theme. So, today, the advantages of MBPC are widely recognised.

2.2 Typical applications

Model Based Predictive Control has a set of characteristics that make it well suited for industrial control of continuous processes. It is important to note that in the case of petrochemical or paper industry applications the need is to operate close to constraints. Therefore, the constrained MBPC is one of the most attractive techniques for this area. The possibility of including constraints explicitly into the process made MBPC very successful in the industrial world. Handling actuator constraints upon inputs and rates of change in a natural way, this approach enables plants to operate more closely to their profitable limits.
MBPC has been very widely adopted, with over 1000 practical applications worldwide. Other application than process control are in nuclear, steel and automotive industries.
In order to support the above statements we refer to a practical implementation [17] that proved to have the following characteristics:

1. The design and implementation was carried out over a short period of time (three month) including the implementation.
2. No major problems were encountered during operation with full acceptance from the human operator (since 25.02.94).
3. The MBPC has proven to be tolerant to disturbances as it is able to use available degrees of freedom.

2.3 Plant model requirements

Mainly this Section refers to the choice of the plant model within MBPC algorithm in general. Additional specifications for the present challenge will be made within Chapter 3. MBPC can be used with nonlinear models , but faster real time performance requires linear ones.
We assume a linear model in state space form :

$$\begin{aligned} x(k+1) &= Ax(k) + B_u u(k) + B_d d(k) \\ y(k) &= Cx(k) + \nu(k) \end{aligned} \tag{2.1}$$

where $x(k) \in \Re^n$ is the system state vector, $u(k) \in \Re^m$ is the system control input vector and $y(k) \in \Re^p$ is the vector of outputs, all variables being measured at time k. Here $d(k)$ is considered to describe unmeasured state disturbance input and $\nu(k)$ is an unmeasured output disturbance vector. For this design challenge we have assumed no disturbance model (ie. $d(k) = 0$ and $\nu(k) = 0$). This simplification has some consequences for performance which will be commented upon later. It is required that each pair $(A, [B_u, B_d])$ is stabilizable with controllable modes of (A, B_d) being stable and (A, C) is detectable.

2.4 Controller structure

The defining feature of $MBPC$ is the repeated optimisation of a performance objective over a finite horizon extending from a future time (N_1) up to a prediction horizon (N_2) [5]. Figure 2.1 characterises the way prediction is used within the $MBPC$ control strategy. Given a set-point, a reference $r(k+l)$ is produced and used within the optimisation of the cost function (2.2). Manipulating the control variable $u(k+l)$, over the control horizon (N_u), the algorithm drives the predicted output $\tilde{y}(k+l)$, over the prediction horizon, towards the reference.
The future control movement is determined by minimising the cost function:

$$\begin{aligned} J(k) = \sum_{l=N_1}^{N_2} \|(\tilde{y}(k+l) - r(k+l)\|^2_{Q(l)} + \\ + \sum_{l=0}^{N_u} \|\Delta u(k+l)\|^2_{R(l)} \end{aligned} \tag{2.2}$$

subject to constraints on:

- the inputs levels: $u_l(l) \leq u(l) \leq u_u(l)$
  where $k \leq l \leq k + N_u - 1$
- the input rates of change: $\Delta u_l(l) \leq \Delta u(l) \leq \Delta u_u(l)$
  where $k \leq l \leq k + N_u - 1$
- the output (and state) levels:
  $y_l(l) \leq \tilde{y}(l) \leq y_u(l)$ where $k + N_1 \leq l \leq k + N_2$

$Q(l)$ and $R(l)$ are weights independent of time k and the norm $\|.\|_Q^2$ within the cost function is defined as $\|\alpha\|_Q^2 = \alpha^T Q \alpha$. It is assumed that $\Delta u(k) = 0$ for $l \geq k + N_u$. As in [5, 10] the optimisation is carried out using a quadratic program (QP).

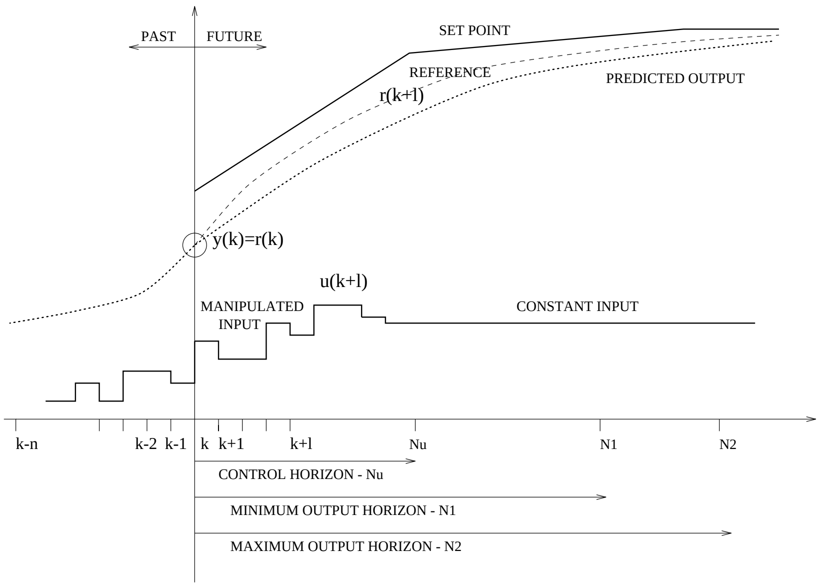

Fig.2.1 Prediction Strategy

The general structure, Figure 2.2, of *MBPC* schemes is the following:

Optimiser contains the constrained cost function and works iteratively in real time. The main task of the optimiser is to compute the present and future manipulated variable moves such that the predicted outputs follow the reference in a desirable manner.

Predictor employing the internal model and the measurement or estimate of the current state provides the optimiser with future predicted values of states and outputs.

Internal model represents the plant. In this paper we use a state-space model for the plant. This is a natural choice for flight control, since the states can be chosen to be physical variables, and this correspondence can be exploited to some extent.

Observer provides state estimates, which can be used in the optimiser.

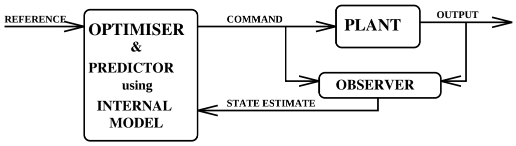

Fig.2.2 The structure of $MBPC$ schemes

2.5 Design cycle description

The design cycle can be performed within a Simulink "test framework" which we have developed. This is shown in Figure 2.3.

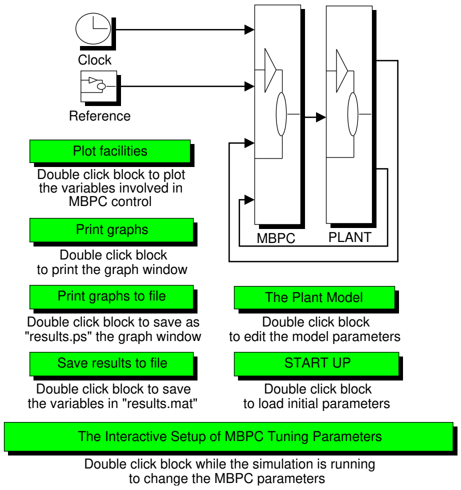

Fig.2.3 The Simulation Framework

The test framework has a flexible user interface with features like parameter tuning and easy plotting of all variables involved in the algorithm. The integration of MBPC with the plant model is the main functional task provided by the test framework. The use of this framework assists the following steps that occur during the design of a MBP controller:

1. Determine the requirements for the closed loop behaviour
2. Produce the internal model of the plant.
3. Define the constraints related to inputs, rates of change in the inputs, outputs and states. Construct matrices that represent these.
4. Choose appropriate dimensions for control and prediction horizons
5. Have a choice of the cost function weighting matrices.
6. Tune the performance of the closed loop system by performing closed loop linear and nonlinear simulations. This involves iteration of steps 3, 4, 5.
7. Perform a stability and robustness analysis.

2.6 A simple design example

A simple SISO design example will give an impression of the use of the MBPC technique. We apply this to an unstable non-minimum phase plant. The transfer function involved is: $T(s) = \frac{-4(s-1)}{s^2-1.6s+4}$ with a zero located at 1 and two unstable poles located at $0.8 \pm 1.833i$. Sampling time was assumed to be 0.2 s. We mention that the control scheme assumed measurable states as well as outputs.
The design steps followed to produce an MBPC controller were the same as the ones presented in Section 2.5. In this particular case the model of the process is the same as the process itself, having the following discrete time state space representation:

```
AA = 1.2791   -0.9179
     0.2295    0.9119
BB = 0.2295
     0.0220
CC = -4   4
DD = 0
```

The Simulink block diagram presented in Figure 2.4 (graph 1) was used to produce responses in the open loop case 2.4 (graph 2). The time domain unit step response shows the well known characteristics of an unstable non-minimum phase process.

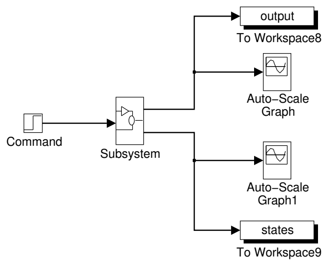

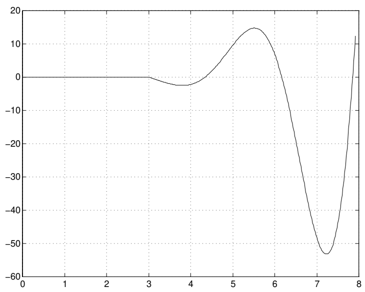

Fig.2.4 Open loop simulation environment and corresponding step response

When tuning we first start to make choices of horizons in order to ensure stability for the closed loop in the unconstrained case. After a trial-and-error process that takes into considerations statements made in Chapter 4 the analysis pushes us towards choosing the following values for control and prediction horizon: $N_u = 8$ and $N_2 = 16$. The horizons choice was made as stated in order to ensure stability of the unconstrained algorithm for step reference trajectories without decreasing dramatically the speed of the on-line optimisation performed, because large horizons mean large matrices involved in the computations. The Figures 2.5, 2.6, 2.7 present simulation results in the unconstrained case that were done as part of the trial-and-error tuning. The graphs sequence follows the design steps towards the final result.

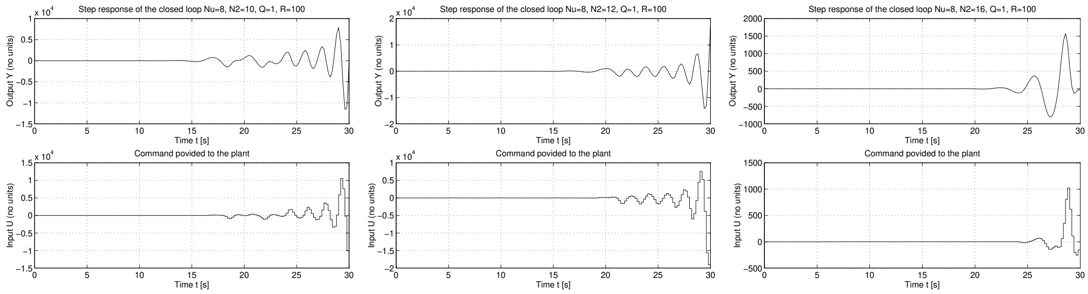

Fig.2.5 Simple design example - The tuning of horizons ($N_u = 8,\ N_2 = 10 \ldots 16$) and weights ($Q = 1$ and $R = 100$)

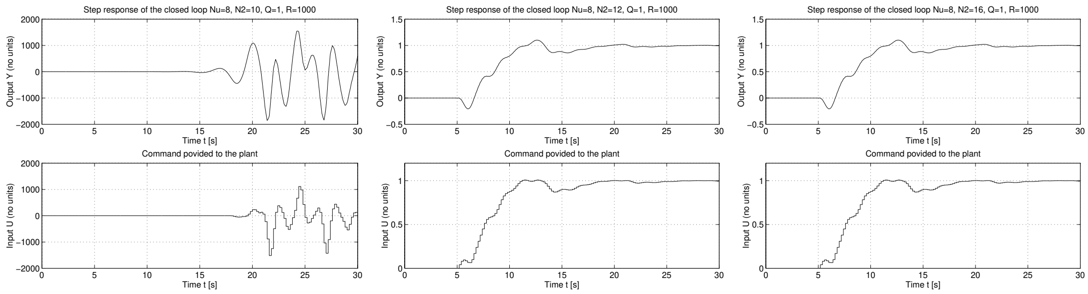

Fig.2.6 Simple design example - The tuning of horizons ($N_u = 8,\ N_2 = 10 \ldots 16$) and weights ($Q = 1$ and $R = 1000$)

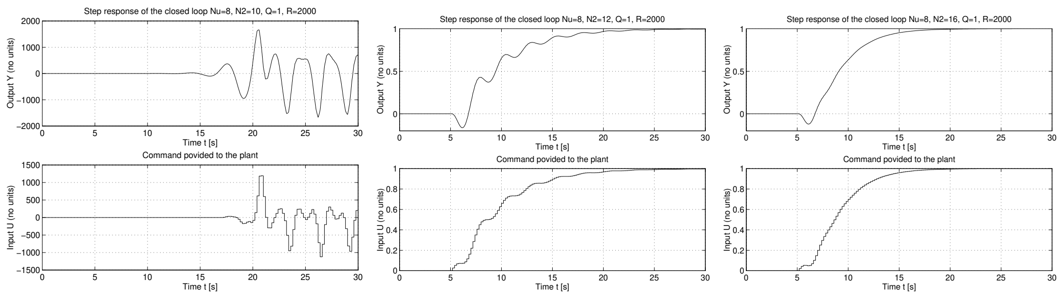

Fig.2.7 Simple design example - The tuning of horizons ($N_u = 8,\ N_2 = 10 \ldots 16$) and weights ($Q = 1$ and $R = 2000$)

The weighting matrix upon the set point has value 1 compared with the one upon input that has the value 2000. Such a choice was motivated by the unstable behaviour of the plant. This choice was found after 5 iterations that increased R weight from 100 to the present value 2000.

The closed loop time response to the step given in Figure 2.7 (graph 3) shows reasonably good performance. An improvement of 5 s in rise time is given if the weight matrix upon the command increment is decreased at the level of 1000 (see Figure 2.6 (graph

3) comparative with 2.7(graph 3)) but, this is achieved with larger movements of the command that involves overshoots.
Second test was to check the noise rejection. Figure 2.8 shows frequency response of the complementary sensitivity function (T) in the unconstrained case (solid) together with the plant (dotted).

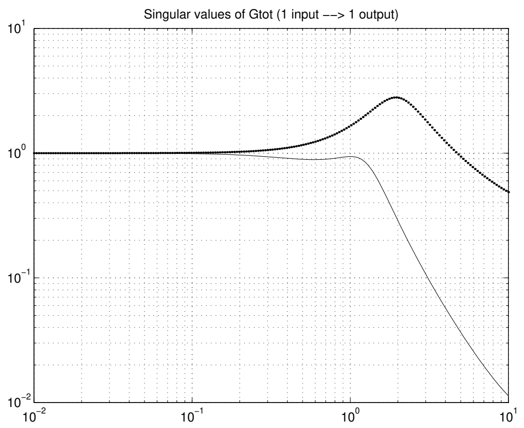

Fig.2.8 Frequency response in the unconstrained case

Second test was to check the noise rejection in the unconstrained and constrained case when we have to track a unit step. When sinusoidal measurement noise with a frequency of 4 rad/s and an amplitude of 0.5 is present in the output measurement the resulting amplitude of the controlled output is 0.15 in the unconstrained case in accordance with Figure 2.8. The response is shown in Figure 2.9 (graph 1 and 2). When the output is constrained to a maximum value of 1 it can be observed that the amplitude of the oscillation remains unchanged but, the mean value is shifted so that the constraint is not violated. The constraint is applied to the output of the MBPC internal model while performing the on-line QP optimisation.

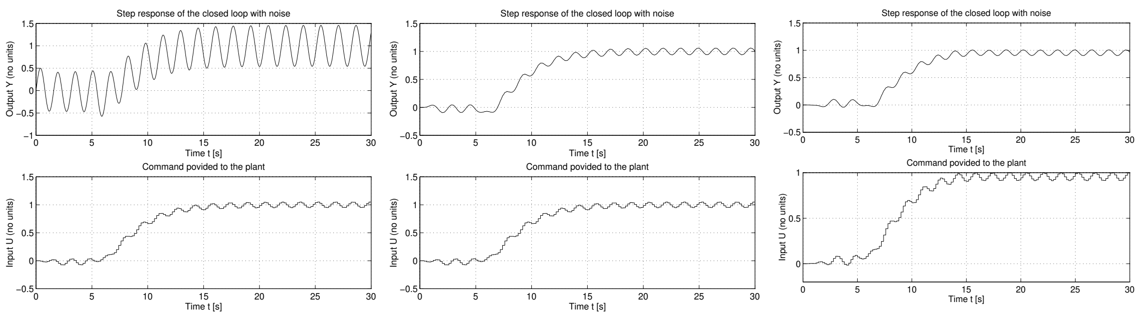

Fig.2.9 Noise rejection - unconstrained and constrained case

3 The selection of the controller architecture for the RCAM problem

In this Section the control system architecture for the overall system will be described. The controller structure we have adopted was a MBPC controller (inner loop) in combination with a H_∞ controller (outer loop). The design consisted of separate design of the inner and outer loops for each of the channels.

Before presenting the measurement, actuators and reference signals involved in control we want to make some remarks about the controller architecture. We have adopted this hybrid structure for several reasons part of them technical and part strategic. Previous design examples from the literature tackle the issue of MBPC control by using such a controller as a single controller but not in conjunction with others. Therefore this design challenge was regarded as a good opportunity to check a different scheme and check its strong and weak points. So, finally we decided to use MBPC in conjunction with H_∞ controller and the RCAM civil aircraft plant. This choice will investigate the limits of MBPC as a SAS (Stability Augmentation System).

Two more problems should be mentioned here. Proceeding to a design that has an inner loop H_∞ controller and including actuator models the number of states that should be measured or estimated in order to use MBPC technique is increased. Moreover the challenge imposes restrictions about the available measurements (no actuator states or outputs are assumed to be measurable). Therefore, the inner MBPC controller does not include the actuator models as part of its internal model. The second problem concerns the available linear model. The liniarization software uses a 9 state aircraft nonlinear model that makes impossible the choice of the altitude as an output of the resulting linear system.

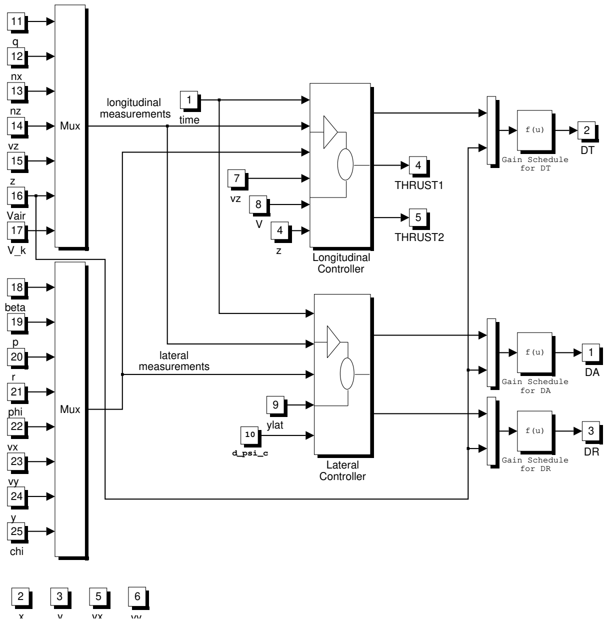

Fig.3.1 The aircraft overall controller structure

Figure 3.1 shows the overall framework making use of separate controllers for each channel. Figure 3.2 show more details of the solution adopted. The approach taken in this design is to split the aircraft controller into two parts: longitudinal and lateral. Each controller is divided into two loops, inner and outer. This approach was used to give the pilot the ability to intervene manually throughout the landing manoeuvre. The behaviour of both inner loop controllers is that of Stability Augmentation System (SAS). These loops were driven by outer controllers providing tracking of main parameters involved in the automatic flight control. All the reference signals for which we ensure tracking by means of the outer controller are shown in Figure 3.1.

3.1 Measurement signals

The choice of measurement signals depends on the quality of available signals. Sensor models are not provided because they are assumed to be perfect (which that makes the usual choice of measurement signals difficult). Like other control techniques MBPC works best when state measurements are available. Therefore the approach to RCAM design challenge assumed a state computation from the output measurements of the nonlinear model instead of state estimation. Such a computation is possible under the assumption that the model is perfect. This will be reconsidered at the implementation stage. In our future research an estimation of states will be employed to provide a more realistic design. The inner loop will stabilise and augment flying qualities. The outer loop controller in both longitudinal and lateral case is designed taking advantage of H_∞ loop shaping techniques. This is a simple controller that ensure tracking of the altitude in the longitudinal channel and the heading rate in the lateral channel case. Bibliography for the H_∞ loop shaping design is available in references: [15, 14, 13, 12]. This was a reliable method to obtain a good outer controller in terms of performance and robustness. Another approach could be to have a simple PID controller that ensures tracking in both cases. In this report our aim is to present extensively the design of the MBPC controller.
The choice of measurement signals for this controller was made in accordance with the author's flight control design experience in the case of civil aircrafts. The longitudinal inner controller uses pitch rate (q), air speed (V_a), vertical rate ($\dot{z}$) as feedback signals in the inner loop. Corresponding internal states of the model are pitch rate (q), pitch angle (θ), velocity in x direction of body axes (u_B) and velocity in z direction of body frame (w_B). The outer loop provides altitude tracking, and uses altitude as an output feedback signal.
The lateral inner controller employs side slip (β) and roll angle (ϕ). States used in feedback are: roll rate (p), yaw rate (r), roll angle (ϕ), and velocity along y axis in body frame (v_B). The outer lateral loop provides tracking for the heading angle rate ($\dot{\psi}$) and the horizontal flight path using its measured lateral deviation (y_{lat}).

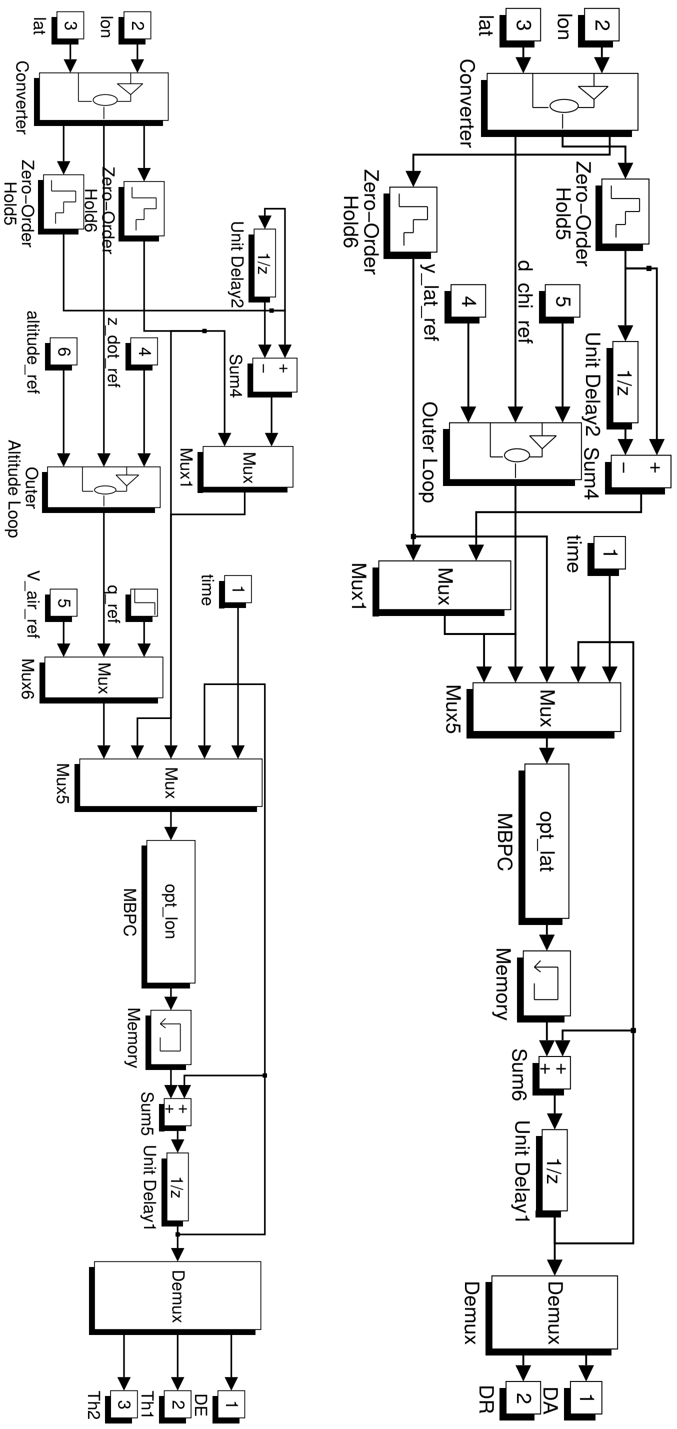

Fig.3.2 The aircraft longitudinal and lateral controller structure

3.2 Actuator signals

Control effectors, well described in the RCAM manual [2], are the following:

- Actuators used to control the longitudinal aircraft channel are the tail-plane (δ_T) and the engine commands (δ_{Th1} and δ_{Th2}). Constraints involved in the optimisation algorithm are saturation of actuators and actuator rate limits (see table 3.1):

Limits	Constrained Variable Name	Unit
$-0.436 \le \delta_T \le 0.174$	saturation of tail-plane deflection	rad
$-0.261 \le \dot{\delta_T} \le 0.261$	rate limits of tail-plane deflection	rad/s
$0.009 \le \delta_{Th} \le 0.174$	engines throttle limits	rad
$-0.028 \le \dot{\delta_{Th}} \le 0.028$	engine throttle slew rates	rad/s

Table 3.1 Longitudinal channel actuator constraints

- The lateral channel is controlled by means of the rudder (δ_R) and ailerons (δ_A). Within the lateral channel MBP controller constraints correspond to saturation of actuators and actuator rate limits (see table 3.2):

Limits	Constrained Variable Name	Unit
$-0.436 \le \delta_A \le 0.436$	saturation of aileron deflection	rad
$-0.436 \le \dot{\delta_A} \le 0.436$	rate limits of aileron deflection	rad/s
$-0.523 \le \delta_R \le 0.523$	saturation of rudder deflection	rad
$-0.436 \le \dot{\delta_R} \le 0.436$	rate limits of rudder deflection	rad/s

Table 3.2 Lateral channel actuator constraints

We have assumed an independent control of these channels by means of the respective actuators (see Figure 3.2). This is justified by the model analysis performed in the following Section 3.3 which provided us with information regarding the coupling level between the lateral and longitudinal channels.

3.3 Models

The plant model, as described in the RCAM Design Challenge Manual [2], is a full six degree of freedom nonlinear model generated as a MEX file by Dymola from an accurate mathematical model of an experimental transport aircraft.
The model used within the MBPC algorithm to generate the control law is a linearised representation of the full six degrees of freedom nonlinear model. This model approximates the behaviour of the nonlinear model (see Figures 3.3, 3.4). The nonlinear model having

Symbol	Input Variable Name	Unit
δ_A	aileron deflection	rad
δ_E	elevator deflection	rad
δ_R	rudder deflection	rad
δ_{Th_1}	engine 1 throttle position	-
δ_{Th_2}	engine 2 throttle position	-
Symbol	State Variable Name	Unit
p	roll rate	rad/s
q	pitch rate	rad/s
r	yaw rate	rad/s
ϕ	roll angle	rad
θ	pitch angle	rad
ψ	yaw angle	rad
u_B	velocity in body axis x direction	m/s
v_B	velocity in body axis y direction	m/s
w_B	velocity in body axis z direction	m/s
Symbol	Output Variable Name	Unit
q	pitch rate	rad/s
n_x	horizontal load factor	-
n_z	vertical load factor	-
w_V	velocity in vehicle carried system along z direction	m/s
z	height	m
V_c	calibrated air speed	m/s
V	total velocity	m/s
β	side-slip angle	rad
p	roll rate	rad/s
r	yaw rate	rad/s
ϕ	roll angle	rad
u_V	velocity in vehicle carried system along x direction	m/s
v_V	velocity in vehicle carried system along y direction	m/s
y	position in earth fixed frame	m
χ	flight path heading angle	rad
Symbol	Simulation Variable Name	Unit
ψ	yaw angle	rad
θ	pitch angle	rad
α	angle of attack	rad
γ	flight path angle	rad
x	position in earth fixed frame	m
n_y	lateral load factor	-

Table 3.3 Inputs, States and Outputs of the linear model

the inputs, states and outputs presented in table 3.3 was linearised around an operating point situated in the middle of the flight envelope, see table 3.4.

Variable Name	Trim Value	Unit
mass	120000	Kg
centre of gravity	[0.23 0.0 0.0]	-
airspeed	80	m/s
flight path angle	0	rad
heading angle	0	rad
initial position	[0 0 -1000]	m
delay	0	sec
gust scale length	150	m
deviation gust	1.5	m/s
constant wind speed	[-10 0 0]	m/s

Table 3.4 The operating point trim parameters

The design uses only this liniarization in order to demonstrate the robustness of the controller for the whole flight envelope. Moreover the lack of actuators model within the internal model of MBPC will show the ability of the control technique to cope with mis-modelling problems.

The decoupling into longitudinal and lateral channels of the aircraft model was performed based on our experience regarding flight control systems for civil aircraft. The level of coupling in between channels, analysed using the full nonlinear model, was proved to be small. The analysis was carried out by providing steps in the commands and checking the cross coupling between channels. The small level of coupling is a general characteristic for a commercial aircraft supporting the decision of splitting the aircraft dynamics in two distinct loops. The linear internal models for the MBPC control were obtained in two stages: first using the full nonlinear model a linear model was produced, then a selection of the corresponding model was employed for each channel based on the decoupling in between channels.

For the longitudinal channel the model is:

```
AS =  -0.9825    0.0000   -0.0007   -0.0161
       1.0000         0         0         0
      -2.1937   -9.7758   -0.0325    0.0743
      77.3570   -0.7675   -0.2264   -0.6684
BS =  -2.4379    0.2912    0.2912
            0         0         0
       0.1837    9.8100    9.8100
      -6.4785         0         0
CS =   1.0000         0         0         0
            0  -79.8667   -0.0283    0.9996
            0    0.0000    0.9996    0.0290
DS =     0     0     0
         0     0     0
         0     0     0
```

The eigen values of the AS matrix:

	real	imaginary	frequency	damping
(1)	-0.01139	-0.1264	0.126	0.0897
(2)	-0.01139	0.1264	0.126	0.0897
(3)	-0.83029	-1.1069	1.383	0.6000
(4)	-0.83029	1.1069	1.383	0.6000

In addition we provide a brief analysis of the dynamics of this model in terms of flight dynamics. Hence, the two modes that characterise the longitudinal channel are phugoid (1,2) and short period (3,4) (time responses are shown in Figure 3.3).

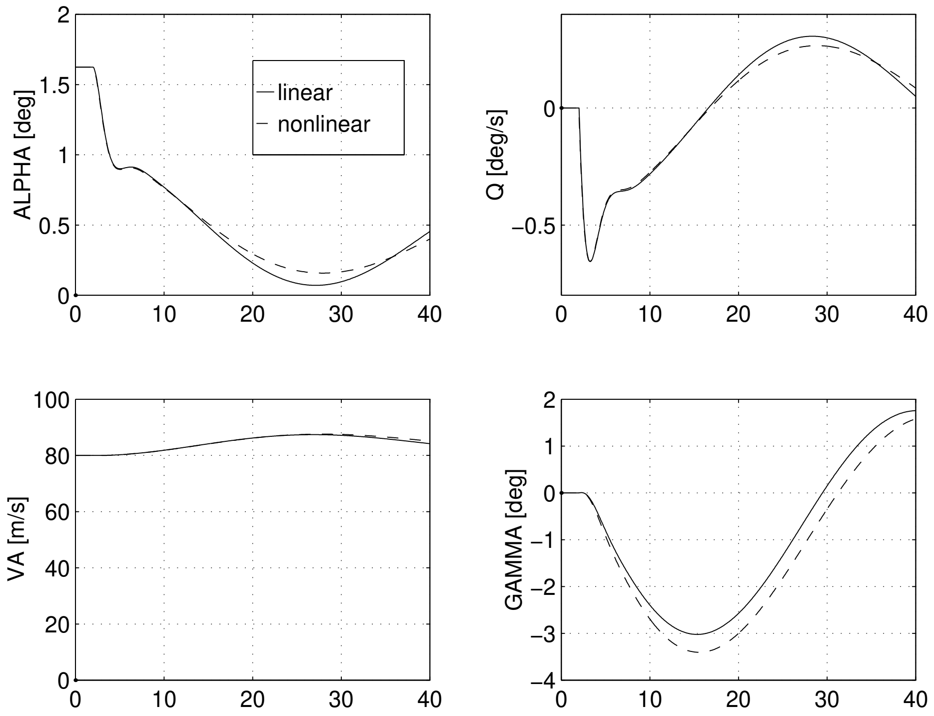

Fig.3.3 Time responses of the longitudinal channel linear model

Developing a similar analysis for the lateral channel we end up with the model:

```
AS =   -1.2667    0.5498    0.0000   -0.0242
        0.0522   -0.5207   -0.0000    0.0045
        1.0000    0.0283   -0.0000         0
        2.2667  -79.9679    9.7897   -0.1699
BS =   -0.8402    0.2904
       -0.0176   -0.3325
             0         0
             0    2.0384
CS =         0         0   -0.0000    0.0125
             0         0    1.0000         0
DS =     0     0
         0     0
```

The eigen values of the AS matrix:

	real	imaginary	frequency	damping
(1)	-0.183	0.0000	0.1836	1.0000
(2)	-0.235	-0.5954	0.6404	0.3684
(3)	-0.235	0.5954	0.6404	0.3684
(4)	-1.301	0.0000	1.3017	1.0000

characterised by the following modes: lateral (4), spiral (1) and Dutch roll (2,3) having the corresponding time responses shown in Figure 3.4.

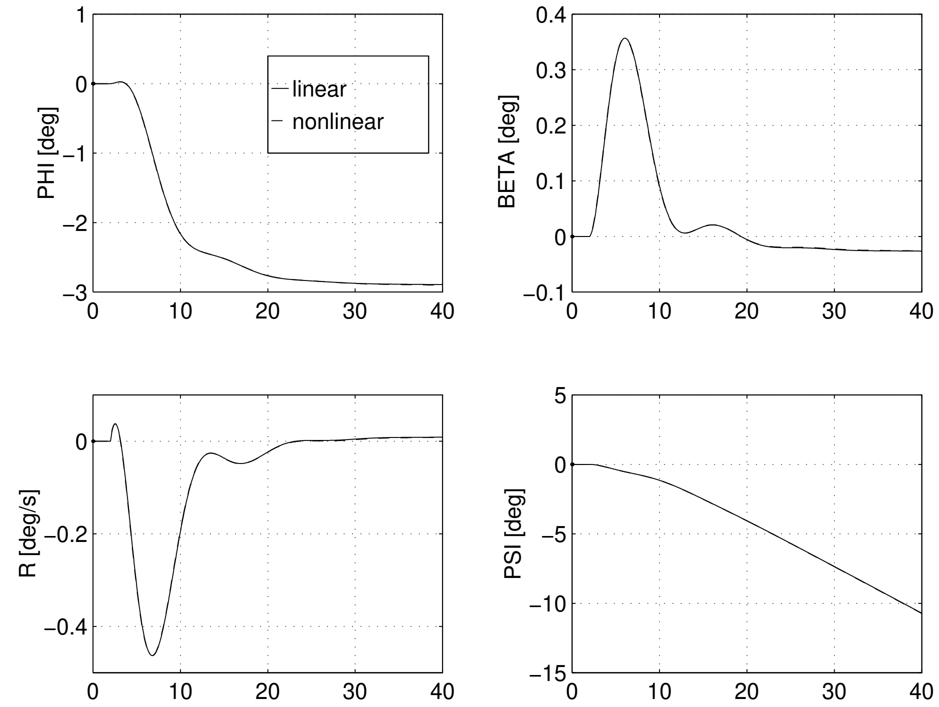

Fig.3.4 Time responses of the lateral channel linear model

As stated, in order to prove some of the features of the MBPC algorithm, such as constraints handling and adaptability, we are not going to use an augmented model containing actuator or delay models. Therefore, instead of using the actuator models we prefer to specify their characteristics and bandwidth via constraints.

3.4 Reference signals

During automatic flight control references for the controller are generated primarily based on time rather than on geometrical information. Therefore time is used as an independent variable for parameterising the trajectory. Effectively, this implies the possibility of a smooth transition from 3D to 4D scenarios. In the actual trajectory generator the time exists as an internal state. At each integration step the aircraft position is compared with the desired one, resulting in an “along the track error”, a parameter of importance in 4D navigation. Once the aircraft moves away from the desired trajectory due to disturbances or poor controller performance the time error (simulation base time minus the aircraft time along the track) computed will act as an extra reference signal.

The trajectory generator provides following outputs, mostly given in earth frame: x_E, y_E, z_E - desired position vector, u_E, v_E, w_E - desired velocity vector, V_E - modulus of total velocity, y_{lat} - lateral deviation from the horizontal flight path and $\dot{\psi}$ - heading angle rate. Other outputs refers to delay time resulting from deviations from the desired trajectory and engine failure or wind generator. All signals used as references are consistent despite a certain redundancy.

In our design we use all these signals in order to ensure the fly by wire facilities as well to provide a possible command to the pilot by conventional means: commands given to the MBPC controlled aircraft. For the longitudinal channel the MBPC controller is provided with the following reference signals: pitch rate (q), air speed (V_a), vertical rate ($\dot{z}$). The lateral controller has following references provided: side slip (β) and roll angle (ϕ).

Most MBPC schemes assume knowledge of the future set point. In this case we employed MBPC as a SAS. In this report we have employed MBPC as a SAS for which no knowledge of the future set point sequence is assumed. The reference trajectory is generated assuming that current set-point (at time k) will be maintained over the whole prediction horizon ($r_i(k) = \cdots = r_i(k+l) = \ldots r_i(N_2)$). Figure 2.1 presents in detail the meaning of set-point vs. reference. In our particular case the plant is a transport aircraft therefore such an assumption can be maintained because of the slow set-point variation from one discrete time step to another. The set-point is provided either by the pilot or by the outer loop controller.

In general the generation of the reference trajectory assumed a certain knowledge of the set-point to be followed. In our particular case the reason we construct as shown above the future set point is the lack of a priori information. For other types of applications using MBPC this issue has to be reconsidered. Another way to generate the reference trajectory is via a filter such as: $r(k) = y(k)$, $r(k+l) = \alpha r(k+l-1) + (1-\alpha)s(k)$ where $y(k)$ is the current output, $s(k)$ is current set-point at time k for $l = 0 \ldots N_2$ and $\alpha \in [0,1]$. When $\alpha = 0$ we obtain $r_i(k) = \cdots = r_i(k+l) = \ldots r_i(N_2)$ for $l = 0 \ldots N_2$ which is the case considered in the report.

In our particular design challenge the plant is a transport aircraft therefore such an assumption can be maintained because of the slow variation of the command from one time step to another. The command is provided either by the pilot or by the outer loop controller. The way we generate the set point assumes that it is reached within the control horizon and the performance parameters are met within the prediction horizon. It is important to note that no terminal constraints are used during the optimisation.

The filter which generates the reference from the set-point can be regarded as another design variable whose effect is approximatively equivalent to the manipulation of weights but more convenient for the designer in some cases.

4 The translation of RCAM design criteria into method dependent objectives

The RCAM design criteria are set up in method independent terms in Section 3.2 of the RCAM manual [2]. This Chapter considers these requirements and provide a procedure to approximate them by means of objectives compatible with the MBPC design methodology. Before starting the presentation of the translation of RCAM design criteria into method dependent objectives it is well to have defined the performance and robustness concepts. Two types of performance can be distinguished: servo and regulator performance. Several aspects of the servo behaviour of a closed loop system can be measured by using a step as the reference trajectory. Figure 4.1 shows the variables involved in the servo performance definition:

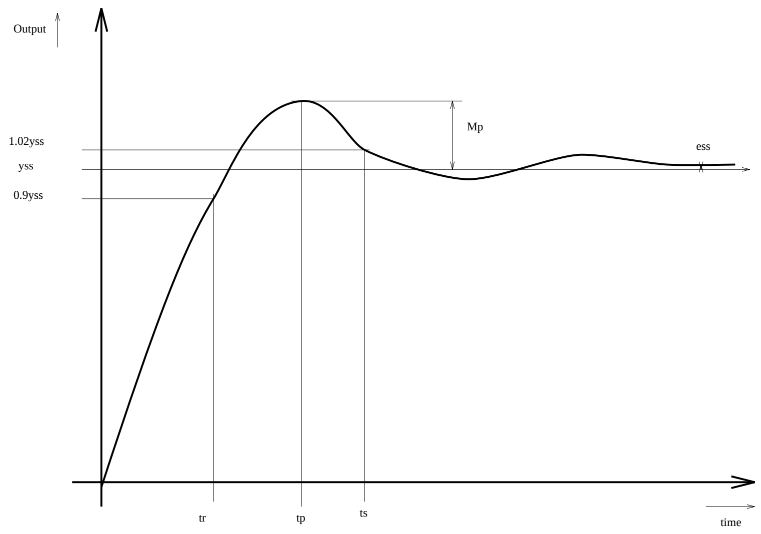

Fig.4.1 Servo performance criteria

These variables are:

rise time (the time required for the system to reach 90 % of the input value): $t_r = \min_t(t/y(t) \geq 0.9)$ [s]

peak time (the time in which the response reaches its maximum value): $t_p = \arg\left(\max_t(y(t))\right)$ [s]

settling time (time required for the system to settle within 2 % of its steady state value): $\min_t\left(\frac{t}{|(y(t)-y_{ss})|} < 0.02 \mid y_{ss} \mid\right)$ [s]

the overshoot: $M_p = (y(t_p) - y_{ss}) \times 100$ [%]

the steady state error: $e_{ss} = \mid (1 - y_{ss}) \mid \times 100$ [%]

where y_{ss} represent the steady state value of $y(k)$. The majority of time domain performance requirements are included in the algorithm by means of the tuning parameters.

However, the smaller the sampling period the more accurate will be the servo performance criteria based on discrete time information. It is highly unrealistic that the process model, used within MBPC, is equal to the real process. Hence, it is important to investigate the influence of modelling errors on the properties of the closed loop system.

Main design criteria that are passed direct into the method are the constraints upon actuators (rate and position limits). All the constraints presented in tables 3.1 and 3.2 are included in the method. Safety constraints regarding the minimum or maximum allowable speed and maximum roll angle are formulated as output constraints. Within the MBPC method we have embedded the minimisation of the control effort (ie. the second term in the cost function 2.2). The on-line optimisation will produce a solution with respect to this requirement that can be influenced by using the corresponding weight. Performance criteria defined in the RCAM manual [2] in time domain such as rise time or overshoot (see above definitions) are passed to the control method via control and prediction horizons and weights involved in the cost function definition. The next Section aims to present some of the general tuning ideas. This Section is followed by another one giving the necessary insight to the RCAM design challenge MBPC parameters tuning.

4.1 Design parameter adjustment strategy

In the case of MBPC designs the design criteria are used to tune parameters of the method. These tuning parameters are: control and prediction horizons, weighting matrices, sampling time and sometimes even constraints boundaries. The choice of these parameters is based on several theoretical results, but certain rules of thumb as well, integrated together in a trial-and-error tuning.

4.1.1 Control and prediction horizons

Mainly, the influence of control and prediction horizon is upon the performance of the controlled system but, some influences upon robustness could be seen as well. In general a smaller control horizon makes the controlled system more robust to uncertainties such as parameter variations [16]. In general the choice of these horizons is made in connection with the knowledge of the future set point and the dynamics of the system. In our case there is no knowledge of the set-point.

Therefore, in case of the control horizon we perform a step response analysis of the system assuming a predefined sampling period. Following a trial-and-error tuning we end up with dimensions in between 4 and 8 steps ahead.

The prediction horizon is derived from the settling time, generally having a dimension smaller or equal to 20. Otherwise the speed of the control algorithm will be decreased to an unacceptable extent. An increase of the prediction horizon should be considered when the control system proved to have long settling time. The prediction horizon must contain at least the non-minimum phase behaviour in the case of such systems to be controlled

using MBPC. The robustness of performance and stability impose extra boundaries on control and prediction horizons.
The effect of the prediction horizon upon step responses (via its defining parameters: rising and sampling time) was studied. The influence upon performance is relatively large for a prediction horizon from 1 to 8, but significantly smaller for horizons greater than 8. The control horizon effect upon performance is quite important. The dimensions chosen for this horizon are often in the range 2 to 8.

4.1.2 Sampling period

The sampling period plays an important role in MBPC controllers. This parameter also defines the discrete time state space representation of the continuous time linear model used as reference model within MBPC. A possible choice for this control parameter is ten times smaller than the fastest settling time in the closed loop system (the value of T_s is obtained using the linear time responses analysis). Another restriction for T_s is given by the application (ie. a civil flight control system operates using a sampling frequency in the range 8 – 20 Hz).
There is a tradeoff between decreasing the sampling period and increasing dimensions of matrices involved in the MBPC algorithm or the number of optimisations performed in the time unit. To conclude, if the sample period is small in relation with the servo performance of the system (eg. settling time) this will result in large control and prediction horizons possibly causing numerical problems. However, the smaller the sampling period, the better can a reference trajectory be tracked or disturbance rejected.
As a final remark: it is important to be aware that the sampling time has a strong influence upon all tuning parameters of the MBPC technique.

4.1.3 Weighting matrices

The weighting matrices upon the outputs and control increments are an important design parameter. The matrix that weights the difference between the set point and the plant model output is positive definite, as well as the command increment weighting matrix. Both give a measure of the tracking properties required from the closed loop system.
The control increment weighting matrix gives a measure of the control increment magnitude. This is connected with the stability of the closed loop, in the case of an unstable plant such as in our example. The magnitude of the increment will influence in its turn the servo performance indices so, during the iterative fine tuning we took advantage of this.
At the moment, we have limited theoretical tools to guarantee stability in the case of the constrained optimisation. As a result the first step in the controller design has to be the tuning of the controller in the absence of constraints. Then, a softening mechanism can be employed as in [4], formulation that covers any mixture of hard and/or soft constraints.

We allow a violation of the hard constraint by an amount $\nu \leq 0$. Next, we add to the cost function 2.2 the term $\| \nu \|_W^2$, where W is the weight that determines the effect of softening: for $W = \infty$ we get hard constraints; $W = 0$ corresponds to a complete removal of the constraints. With respect to the previous statements we have to note that both weighting matrices give necessary tools to avoid constraints violation over the control and prediction horizon, which might cause instability.
The tuning of weighting matrices is not a one step process. At the beginning we tune the weights of the MBPC controller using the time simulations involving the linear model of the plant. This step is followed by fine tuning done by time simulations employing the full nonlinear model of the plant. This tuning is another example of a trial-and-error procedure involved in choosing the MBPC controller parameters. The small time step of the integration method that we are forced to use because of the discrete time simulations makes this a time consuming process, but this is specific to the Simulink simulation software.

4.1.4 Set point generation

The shape of the set point represents an indirect tuning parameter for MBPC schemes. Because for this design challenge the approach taken was to use MBPC controllers as inner loop stability augmentation systems a priori knowledge of the set point was not assumed. Section 3.4 provides us with information regarding the way the set-point over the prediction horizon was defined and the corresponding reference trajectory to be followed. Other choices for the generation of the set-point from the present command can be used, but those should be linked with the model dynamics.

5 The description of the design cycle

In this Chapter, following the procedure presented in Section 2.5, a description of the necessary actions that were taken for each iteration within the design cycle will be given. In order to produce the model required within MBPC algorithm we linearised the nonlinear aircraft model excluding sensors, actuators and time delays around an operating point at the middle of the flight envelope. This model was linearised using inputs outputs and states defined in Section 3.3. Then the problem was split in two separate channels: longitudinal and lateral. For each channel the inner loop was analysed and a controller designed. Various responses mentioned in the manual were checked using linear model as an intermediate analysis. The design for the outer loops was achieved using a linear time invariant representation of the MBPC controller, namely in the unconstrained case. The aircraft linear model was augmented with LTI controller in order to produce the model required in H_∞ loop-shaping method. The next step was to perform a more extended analysis of the inner and outer loops using simulations involving the full nonlinear aircraft model. This helped us to get a fine tuning of the MBPC controller, process that was done in few iterations. The first design was achieved for the longitudinal channel. This gave useful experience for designing the lateral channel. Therefore the time involved in the inner lateral channel MBPC controller design was shortened by a considerable amount. The fine tuning of this controller when full nonlinear model simulations were done took the same amount of time as in the longitudinal case.

5.1 Numerical tools for controller synthesis and analysis

In order to perform synthesis and analysis in the MBPC case, a particular test bed has been developed. The test framework involved is presented in Figure 2.3. This test bed was included in the controller block of the RCAM design framework (see Figure 5.1). Various variables are taken out to the Matlab workspace in order to help design procedures. The integration of MBPC with the plant nonlinear model is the main functional task that the test framework performs. The major novelty in this Simulink framework is that it includes a controller that performs an on-line optimisation. Therefore several problems that occur involving delays and synchronisation between functional blocks were solved using built-in, but undocumented, Simulink features used for multi-rate discrete time systems. This test bed is now the basis of a Matlab-Simulink Model Based Constrained Predictive Design Space providing, in the user interface, all facilities required for MBPC design.

The heart of the MBPC algorithm consists of an optimiser, involving the quadratic programming algorithm, that provides the control increment for the next step. Setup programs perform the parameter definition and tuning and prepare the optimisation to be carried out at any discrete time instant. Script files of these programs are presented in annex A.

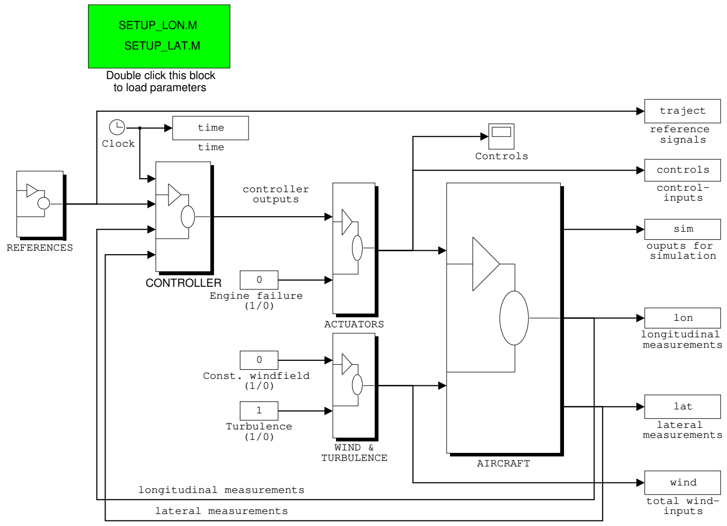

Fig.5.1 The Simulation Framework for the linear aircraft system

5.2 The tuning of MBPC parameters in the RCAM challenge model

5.2.1 Longitudinal channel

Using the strategy presented in the Section 4.1 we have to take into consideration requirements regarding: the flight path angle response (vertical rate response), the altitude response and the cross coupling between altitude and airspeed in order to tune the MBPC parameters.

The choice of the control horizon was made by increasing it from a value of 4 (the model order), the minimum value recommended in [16], trading off reduction in control surface activity against computational complexity. The final value chosen was $N_u = 8$.

The tuning of the prediction horizon was made with respect to the settling time in the airspeed response for a step of 13 m/s in airspeed command. A small prediction horizon provides large gain in the constrained case. Disturbances can lead to constraint violations which can in turn lead to instability. We started with a prediction horizon $N_2 = 15$ and found that this value gave instability in the presence of vertical wind shear. Trading off the computational complexity against stability we have increased N_2 and finally set it to a length $N_2 = 18$.

At the beginning of the design procedure the sampling time for the MBPC controller was set to 0.1 s (a sampling frequency of 10 Hz). This was made for the following reasons: 1) the dramatic increase of the simulation time owing to the small time step in the integration method and 2) a sampling frequency of 10 Hz was proved to be still at the bottom of the range used in civil aircraft industry (in this case the aircraft is assumed to be a rigid body all the higher modes being treated as uncertainties).

The choice of the weighting matrices was made in order to fulfil following requirements:

1) to track in a good manner the commands provided by the outer loop 2) to minimise the control effort and to improve stability. In accordance with the internal model dimensions $Q = diag(1, 1, 1)$ and $R = diag(1 \times 10^5, 7 \times 10^5, 7 \times 10^5)$.

The reference to be followed by the output was constructed from the set-point under the assumption of a priori unknown commands, a realistic expectation for the MBPC used as a Stability Augmentation System (SAS).

5.2.2 Lateral channel

The lateral channel MBPC controller was tuned mainly by translating RCAM design challenge requirements such as roll angle response, side-slip angle response, heading rate response and lateral deviation response into the tuning parameters specific for the method.

As in the longitudinal case we have fixed from the beginning a few of the parameters such as: $T_s = 0.1$, $N_u = 8$ and $Q = diag(1, 1)$. The tuning involved the other parameters in a trial-and-error process. The prediction horizon was tuned first with respect to the settling time requirements for the side-slip response. The final choice was $N_2 = 18$. When tuning N_2, in parallel, the input weighting matrix was adjusted up to the final values of $R = diag(20, 60)$. This choice provides the performance specifications of the roll and side-slip response to be consistent with the RCAM design challenge manual and reduces the lateral deviation error to 0 quickly enough.

We found that in order to meet the specification during the engine failure we had to increase the prediction horizon up to values of $N_2 = 22$. The way the set-point and the corresponding reference to be followed by the predicted output were constructed is completely similar as in the longitudinal channel case.

5.3 Linear analysis

In order to perform the fine tuning of the MBPC controller (design step 6) various responses were calculated and compared to the requirements in the RCAM design challenge manual.

5.3.1 Longitudinal channel – inner loop

The plant used for control was the linear model of the aircraft. Within the MBPC the discrete time representation of this model was employed as the internal model. All the results presented were produced using the environment presented in Figure 5.1. For the linear analysis, responses that involved the outer loop controller are not relevant because of the nonlinear inner MBPC controller that made us unable to come up with an accurate augmented linear model of the MBPC controlled plant.

5.3.1.1 Flight path angle response

We subject the system to a step of 3° in commanded flight path angle. The response is shown in Figure 5.2. The tracking ensured is good (rise time of 5 s, settling time 15 s), the overshoot is small (less than 1 %), and the cross coupling to velocity is negligible (less than 0.4 m/s).

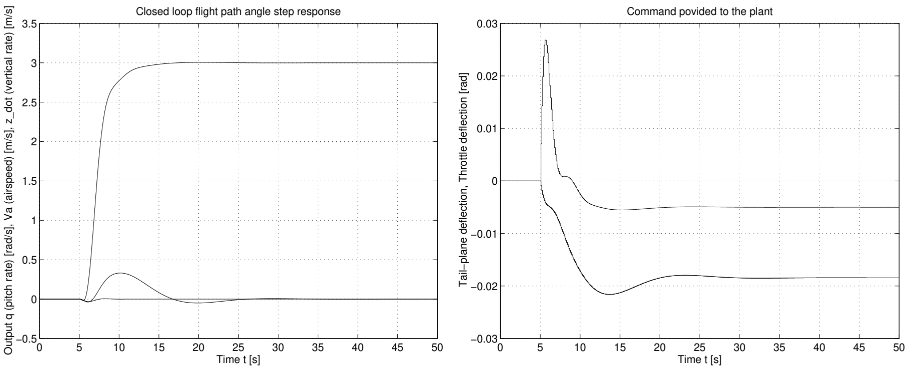

Fig.5.2 Linear system - Flight path angle response

5.3.1.2 Velocity response

The system response to a step of 13 m/s in commanded velocity is shown in Figure 5.3. Most of the requirements were satisfied. The rise time in air speed is around the specified 12 s and the settling time is at about 45 s. The overshoot, due to no a priori information assumed to be available, is 15 %, higher the the specified 5 %. However, the cross coupling to flight path angle is as well a bit higher than the specified 0.5°.

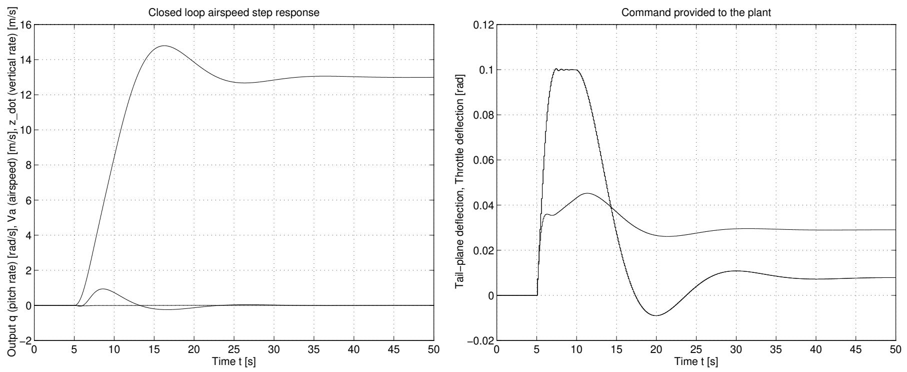

Fig.5.3 Linear system - Velocity response

As the second performance parameter the system response to a step change in airspeed of 13 m/s, caused by a wind shear, was calculated and plotted in Figure 5.4. The flight path angle was perturbed by approximately 4°, which is higher than the specified value on cross coupling from air speed to path angle.

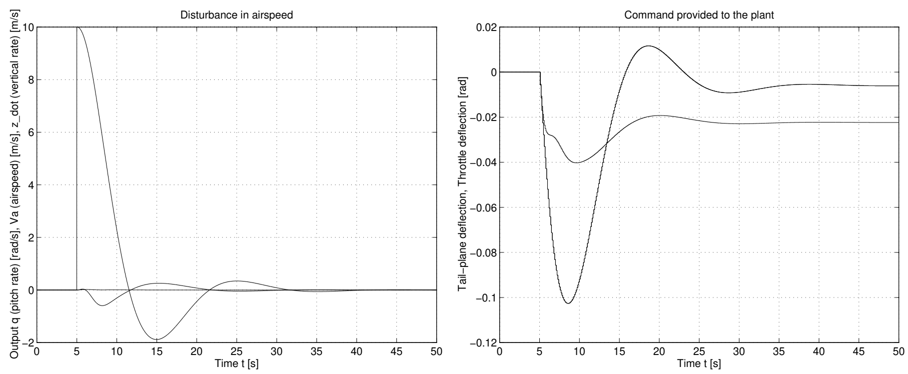

Fig.5.4 Linear system - Air speed response

5.3.2 Lateral channel – inner loop

5.3.2.1 Roll angle response

The response of the system to 0.34 rad (20°) step in the roll angle command is shown in Figure 5.5. The cross coupling from roll to side slip is as required, less than 1°. The tradeoff between a short rise time and a low overshoot or limit upon the aileron rate was solved by employing adequate values for horizons and weighting matrices. The procedure of choosing the values for horizons and weights is described in Section 5.2.2.

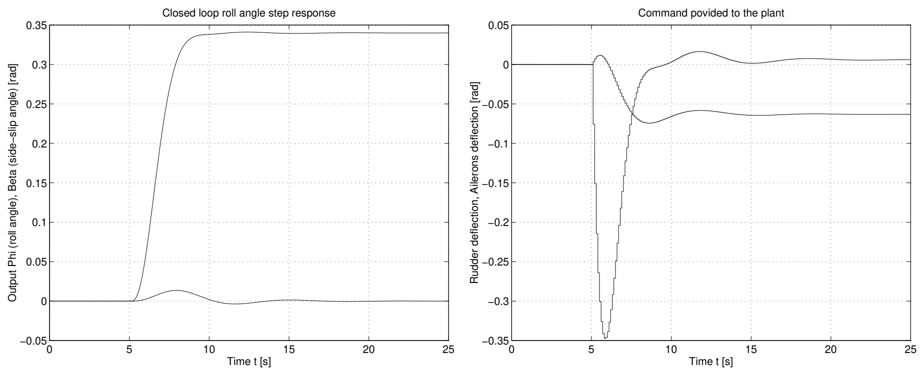

Fig.5.5 Linear system - Roll angle response

5.3.2.2 Side slip angle response

The response in side-slip command of 0.034 rad (2°) is shown in Figure 5.6. Associated commands for ailerons and rudder are presented. The system response is not delayed significantly by introducing the MBPC controller and the rise time is 4 s.

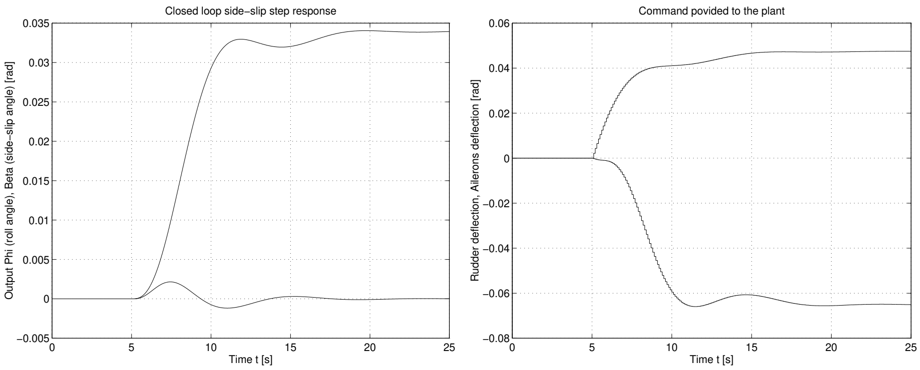

Fig.5.6 Linear system - Side-slip response

5.4 Tabular analysis of the results achieved with the linear plant

Channel	Responses	Performance requested	Performance achieved	Decision
Longitudinal	flight path angle	$t_r < 5s$, $t_s < 20s$ $M_p < 5\%$	$t_r = 3s$, $t_s = 12s$, $M_p = 0\%$	+,+,+
	velocity	$t_r < 12s$, $t_s < 45s$, $M_p < 5\%$	$t_r = 12s$, $t_s = 35s$, $M_p = 15\%$	+,+,−
Lateral	roll angle (not specified)	$cross - coupling < 1°$	$cross - coupling = 0.8°$	+
	side-slip angle	$t_r < 5s$, $t_s < 20s$, $M_p < 5\%$	$t_r = 3s$, $t_s = 12s$, $M_p = 0\%$	+,+,+

Table 5.1 MBPC controlling the linear plant – analysis results

6 Analysis of the resulting MBPC controller

The principal analysis method used in the case of MBPC algorithms is time domain simulation. In this Section all simulations have been performed using the nonlinear model. Those using the linear model were studied in Section 5.3. The purpose of this analysis is to make clear to what extent the controller satisfies the design objectives formulated in the RCAM Design Challenge Manual [2].

6.1 Longitudinal channel – inner loop

6.1.1 Flight path angle response

Altitude tracking ensured by the longitudinal outer loop relies on performance characteristics of the flight path angle response (vertical rate response). Therefore, in the first graph of Figure 6.1 we show the behaviour of the nonlinear aircraft (longitudinal channel) when we subject the system to a step demand of $3°$. The step occurred 10 s after the simulation was started in order to avoid influence of simulation transients. The rise and settling time met the specifications ($t_r < 5s$ and $t_s < 20s$). A small overshoot can be observed as a way to improve the rise time in order to ensure better altitude tracking performance. The altitude, as shown in the the second graph of Figure 6.1, is influenced by this constant rate of descent. Both engines are reduced by the MBPC controller to the minimum thrust but this is not enough to maintain the airspeed steady state error at zero.

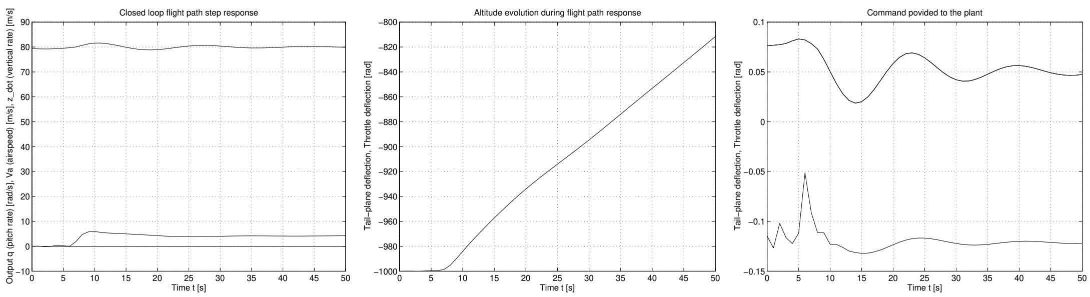

Fig.6.1 Nonlinear system - Vertical rate response

6.1.2 Airspeed response

The velocity response of the nonlinear aircraft model controlled by MBPC is shown in Figure 6.2. The controlled system's speed was subject to a step of 13 m/s (occurring at 5 s after the start of the simulation). The rise time of 10 s and the settling time of 25 s are within the RCAM manual specifications. The overshoot is less than 5 %. The control movement, shown in the second graph of Figure 6.2 has a satisfactory behaviour across the whole manoeuvre. From the first graph of Figure 6.2 it can be seen that no significant cross coupling to vertical rate was shown.

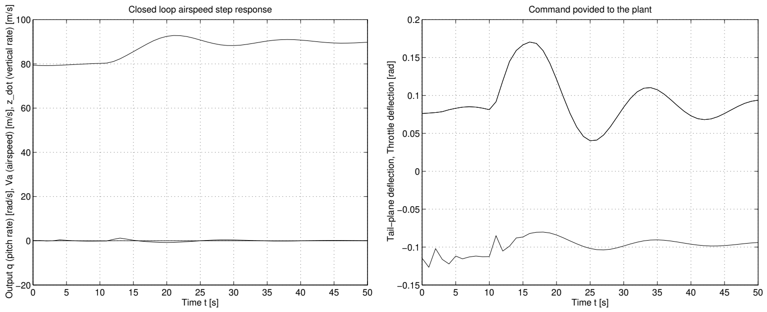

Fig.6.2 Nonlinear system - Speed response to a step demand of 13 m/s

The system response of the nonlinear system to a step change in airspeed of 13 m/s, caused by wind shear, is shown in Figure 6.3 (the step occurred at 5 s). The resulting response shows that the effect of such a constant disturbance, the wind shear, can be reduced in 15 s with a small coupling to vertical rate. The settling time, which is within the specification, is 35 s. During the wind shear rejection the control movement has a satisfactory behaviour. In the second graph of Figure 6.3 the law provided by the constrained MBPC is presented in comparison with the actuator output.

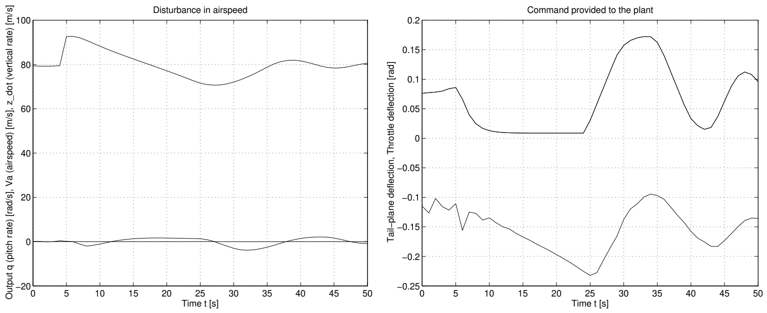

Fig.6.3 Nonlinear system - Step in airspeed

6.2 Longitudinal channel – outer loop

6.2.1 Altitude response

In this report, we present the results obtained in the case of altitude tracking employing MPBC controller as an inner loop controller and an H_∞ controller as an outer controller for a step of 30 m in altitude demand. In this case the closed inner loop will be considered as a block with flight path angle and velocity commands as inputs. The outer loop used for tracking purposes provides us with the responses shown in Figure 6.4. Altitude response is shown in the first graph while the command movement in the second. The tracking ensured by the outer loop in conjunction with the MBP controlled inner loop is within the specifications (the rise time smaller than 12 s and the settling time smaller than 45 s). The overshoot is bigger than the prescribed one of 5 % at altitudes above 305 m.

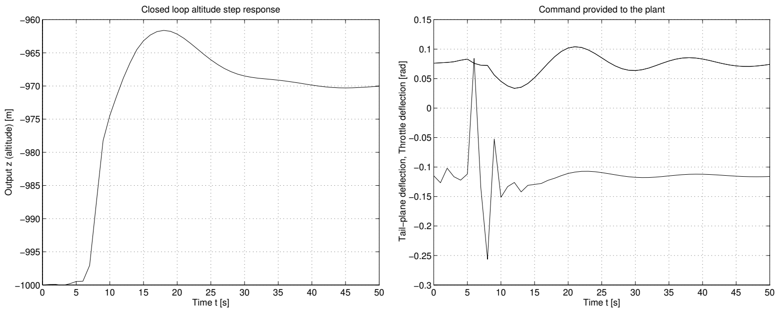

Fig.6.4 Nonlinear system - Altitude step response

6.2.2 Cross coupling between airspeed and altitude

When the velocity step response was simulated the altitude behaviour, shown in Figure 6.5 second graph, respected the manual specifications [2]. These stated that the peak value of the transient of the absolute error between the aircraft altitude and its reference should be smaller than 10 m (see second graph of the Figure 6.5). Conversely for an altitude step of 30 m the peak value of the transient of the absolute error between the aircraft and the commanded airspeed is smaller than 1 kt (see Figure 6.5, first graph).

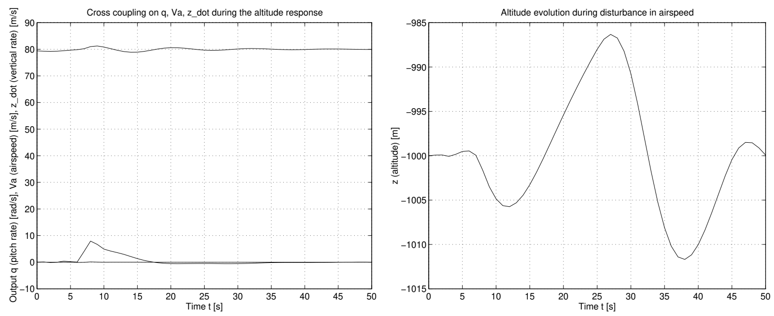

Fig.6.5 Nonlinear system - Cross coupling between airspeed and altitude

6.3 Lateral channel – inner loop

6.3.1 Roll angle response

The roll angle response was analysed by providing the nonlinear system with a step of 0.34 rad (20°)(see Figure 6.6). The rise time of 7 s has proved to be a bit slow when performing a coordinated turn in the horizontal plane. Even though no overshoot can be seen and the settling time is 10 s the response time of the inner loop has to be improved. During the step in roll angle the side slip angle β is small, having peak values below 0.05 rad (1°). In the case of engine failure all specifications were met, as can be seen in Figure 7.2. The specified turbulence conditions still keep the roll angle within bounds (less than 5°). The maximum roll angle is limited using the constrained MBPC algorithm to 30° in order to comply with safety criteria.

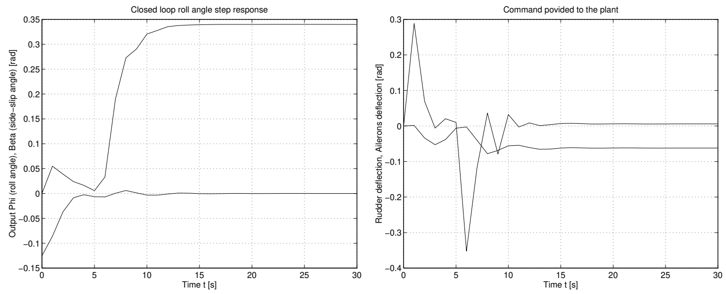

Fig.6.6 Nonlinear system - Step in roll

6.3.2 Side slip angle response

The nonlinear aircraft side slip angle control implemented by MBPC is shown in Figure 6.7 when a step of 0.034 rad (2°) was applied. The rise time of 4 s and the settling time of 25 s comply with the specs. The drawback is in terms of overshoot that is bigger than 5 %. Fortunately the side slip angle control involves small angles, so the overshoot does not cause any problems. Unfortunately there is no overshoot specified in the RCAM manual [2]. The cross coupling to roll angle is less than 0.5°, well below the specified value of 1°.

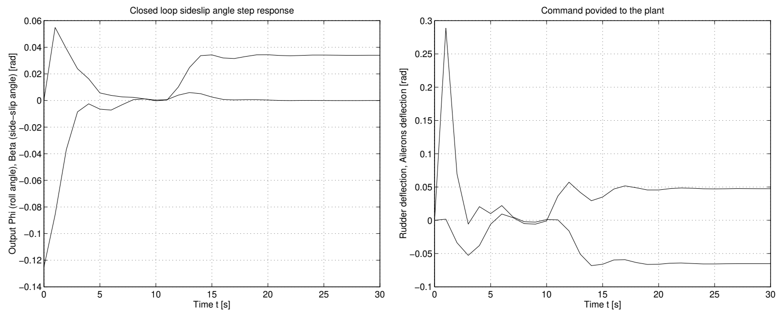

Fig.6.7 Nonlinear system - Step in side-slip

6.4 Lateral channel – outer loop

6.4.1 Lateral deviation

We subject the aircraft to a disturbance step of 20 m in lateral deviation after 5 s. The response (see Figure 6.8, first graph) shows that the error from the desired track is reduced to 10 % in 30 s. The overshoot in the response to the step in lateral command signal at altitudes above 305 m is bigger than the specification, which causes considerable errors when following a reference trajectory that has coordinated turns. There is no steady state error due to constant wind disturbances (Figure 7.4) and the lateral controller copes well with the specified turbulence conditions.

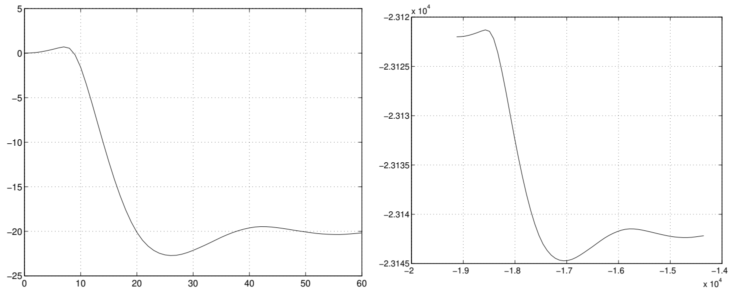

Fig.6.8 Nonlinear system – Response to a lateral deviation of 20 m

6.4.2 Heading rate

As part of the RCAM design challenge requirements we minimise the heading rate in case of engine failure. The results are shown in Figure 6.9, second graph. The heading rate error during lateral Dryden gust is minimised as well. The commanded heading rate is tracked well by the aircraft heading rate, as shown in Figure 6.9.

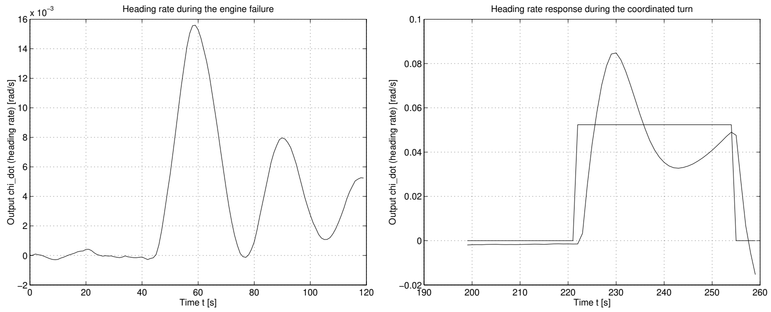

Fig.6.9 Nonlinear system – Response to a step in heading rate of 0.1 rad/s

6.5 Other criteria

As regards robustness analysis, the most significant model uncertainties are: centre of gravity variations, mass variations and time delays. As shown in Section 7.2, controller behaviour is generally satisfactory when the plant involves uncertainties.

Ride quality criteria such as maximum vertical acceleration, maximum lateral acceleration and damping were computed after the evaluation mission was completed, and are presented in table 7.1. Corresponding values across the evaluation procedure (the landing manoeuvre in the absence of gust) are shown in Figure 6.10.

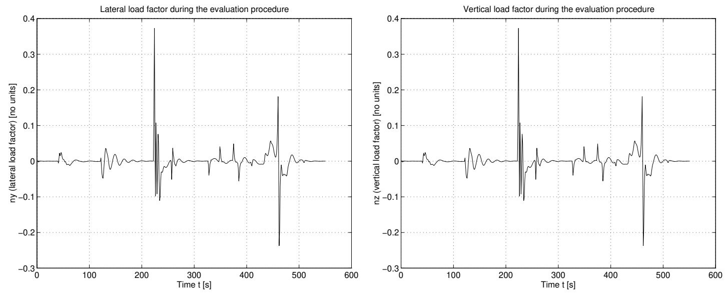

Fig.6.10 Ride quality criteria: lateral and vertical accelerations

All safety criteria specified in the manual [2] were met either because of constraints imposed by MBPC or because of saturation blocks included in the controller outer loops.

The use of MBPC as an inner loop controller keeps the control activity small both for actuators and engines, as seen in Figure 6.11. All units are common in this Figure: *rad*.

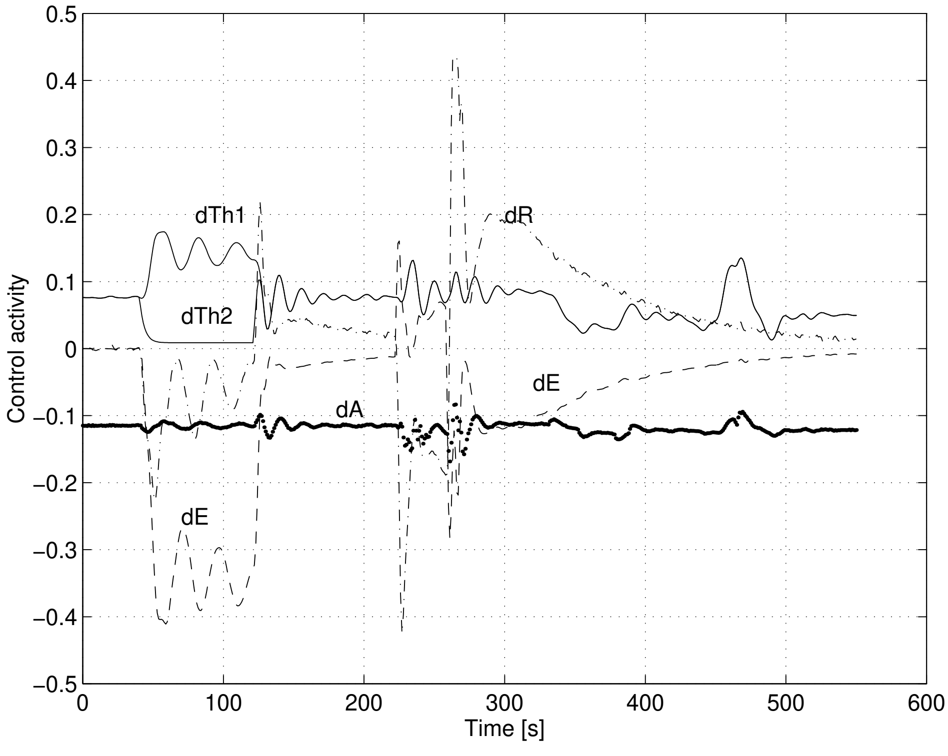

Fig.6.11 Actuators and engines control activity

7 Results of the automated evaluation procedure

7.1 Introduction

This Chapter presents the methodology-independent results of the controller designed in the previous Chapters. It is mostly based on the evaluation mission and scenario defined in [2]: both 'overall tracking performance' and 'inner-loop behaviour' of the controlled system will be evaluated by means of bounds on key variables.The evaluation procedure is fully automated. No changes were made to any of the automatically generated Figures or the table with numerical results.

First a general view of the results will be given in Section 7.2. Next, a more detailed discussion of the behaviour of the controlled aircraft will be based on the four separate flight segments defined in [2]. Finally, a summary of the numerical results of the evaluation will be given in Section 7.7.

7.2 A general view of the results

Before we go into detail on the specific properties of the controller with respect to aircraft behaviour, we will consider a view of the entire trajectory in the 3D plot given in Figure 7.1. In this plot, results are combined with respect to reference trajectory following, disturbance

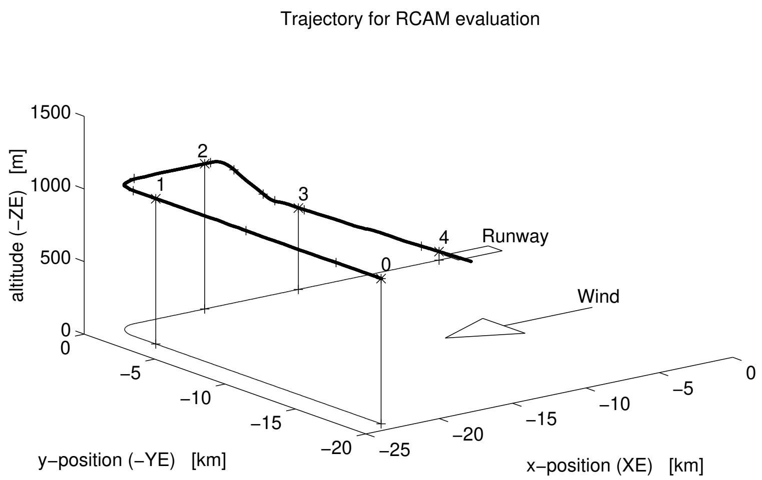

Fig.7.1 The trajectory response of the controlled RCAM model

rejection and robustness. However, the scale is such that deviations from the trajectory should be hardly noticeable. A major robustness demand is taken into account by plotting the four trajectories resulting with nominal, most forward and most aft positions for the centre of gravity. The four trajectories can be seen and evaluated better in the following Figures.

7.3 Segment I: the effect of engine failure

As the RCAM aircraft model is twin-engined, a single engine failure (between points a and b) will mainly result in lateral deviation. Hence Figure 7.2 provides a top view of the first trajectory segment. During the engine failure the dynamic response is acceptable (the roll angle does not exceed 5 *deg*) but the steady state deviation does not return to zero sufficiently quickly (less than 25 *s* after the engine failure) as a result of our omitting a disturbance model (see Section 2.3). The overshoot after the engine reactivation is within bounds. Furthermore, the airspeed does not drop below $1.2 \times V_{\text{stall}}$, which is ensured by the MBPC constrained control.

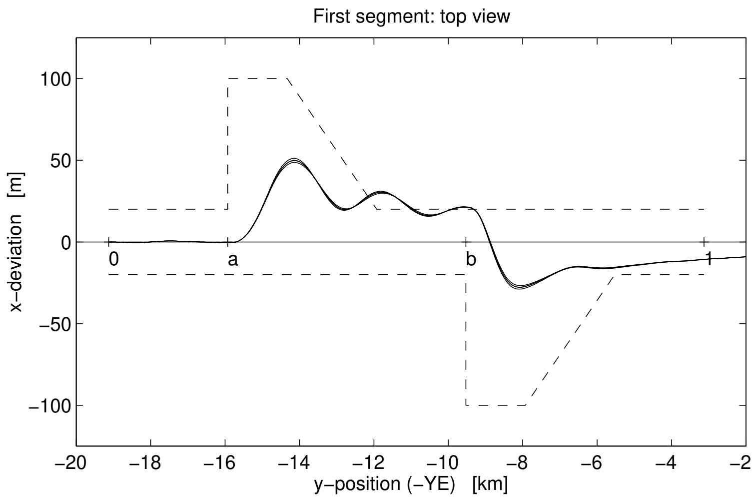

Fig.7.2 Segment I: the effect of engine failure

7.4 Segment II: the 3 *deg/s* turn

At the moment the turn starts, the perfect following of the required trajectory and the desire to perform a coordinated turn would imply a sudden change in the aircraft's bank angle, which is only possible with an infinitely high roll rate. Obviously this is impossible, so that deviations from the desired trajectory at the start (and the finish) of the turn are unavoidable. To demonstrate this, Figure 7.3 gives a top view of the trajectory for all three centre of gravity locations plus bounds within which an acceptable performance should lie. Figure 7.4 provides a closer look at the actual lateral deviations: the bounds are equivalent with those in Figure 7.3.

7.5 Segment III: the capture of the -6 and -3 degrees glide-slope

We start with a glide-slope of -6 *deg*; again it is unavoidable that the aircraft leaves the desired trajectory. It should return to the trajectory without overshoot and well within

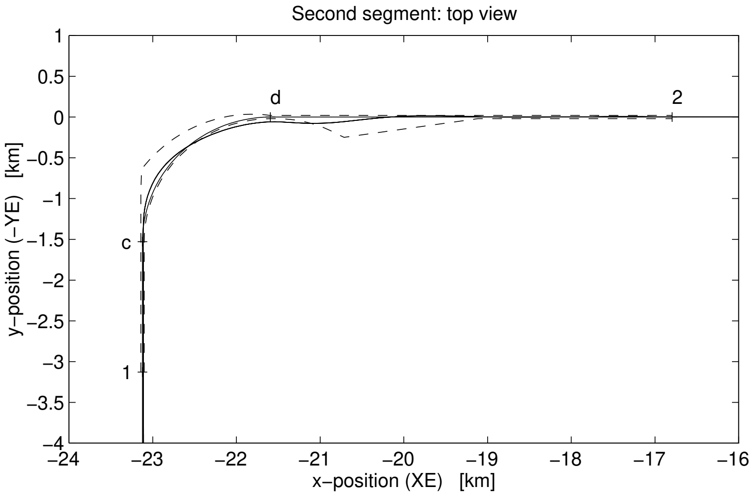

Fig.7.3 Segment II: the 3 deg/s *turn*

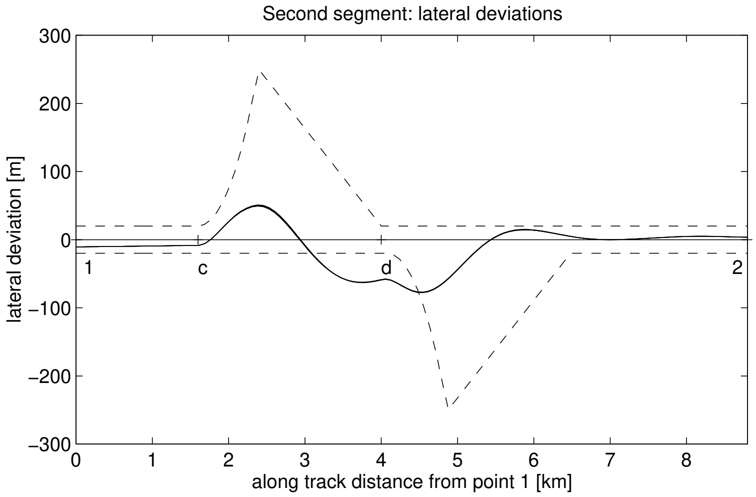

Fig.7.4 Segment II: lateral deviations during the 3 deg/s *turn*

a period of 30 *s*. After that we go to a glide-slope of -3 *deg* such that we get an inverse behaviour with respect to the desired trajectory, that should be about half the size of the first response (if the system has a more or less linear behaviour). In Figure 7.5 the longitudinal response of the aircraft is plotted for three centre of gravity locations and with bounds that specify acceptable behaviour. The vertical deviations from the desired glide-slope are plotted in Figure 7.6.

7.6 Segment IV: the final approach with wind-shear

While on final approach with a glide-slope of -3 *deg* the effect of a wind-shear model is considered. Figure 7.7 shows the longitudinal response of the aircraft for three centre of gravity locations and with bounds that specify acceptable behaviour. The vertical deviations from the desired glide-slope are plotted in Figure 7.8.

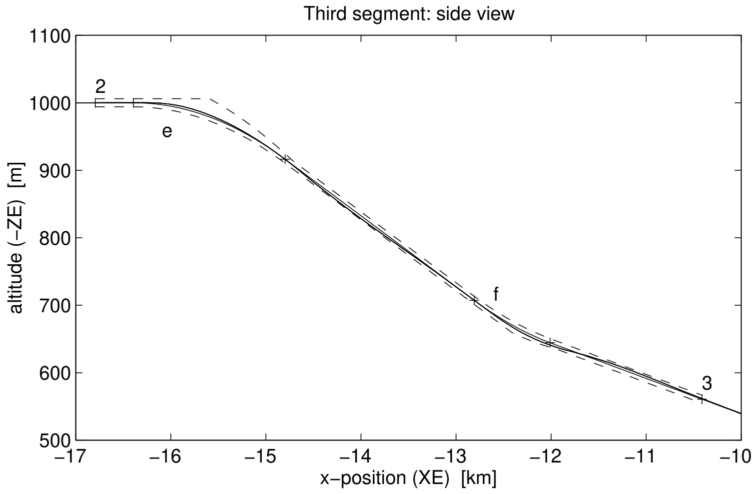

Fig.7.5 Segment III: the capture of the -6 and -3 degrees glide-slope

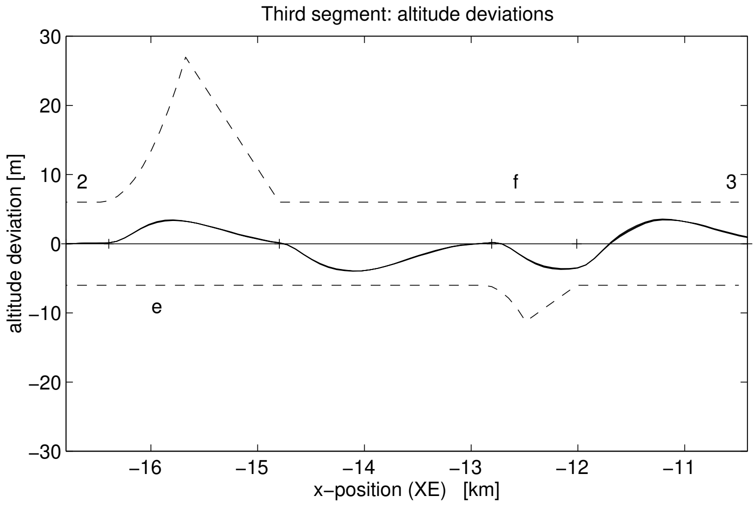

Fig.7.6 Segment III: vertical deviations from the desired glide-slope

7.7 Numerical results

Table 7.1 gives numerical results based on the discussed simulation results. For the motivation and calculation principle of the various results see [2]. Each segment of the evaluation procedure it is considered via the design criteria: performance, robustness, comfort, safety and power. Because the evaluation criteria are independent of the type of controller used the table contains calculable indicators that enable us to obtain an objective comparison between completely different controllers. For each of the above items and for each of the four trajectory segments a single number was calculated.

This number is an important indicator for several aspects of controller performance. In most cases a value smaller than one is acceptable. When saying most cases we would like to point out that in segment II a high roll rate, that is required to meet the given trajectory requirements, will decrease the comfort during this segment, which can be seen

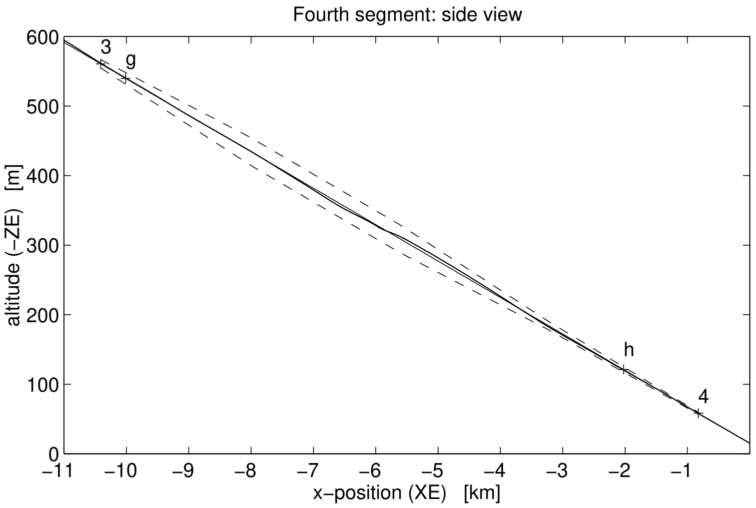

Fig.7.7 Segment IV: the final approach with wind-shear

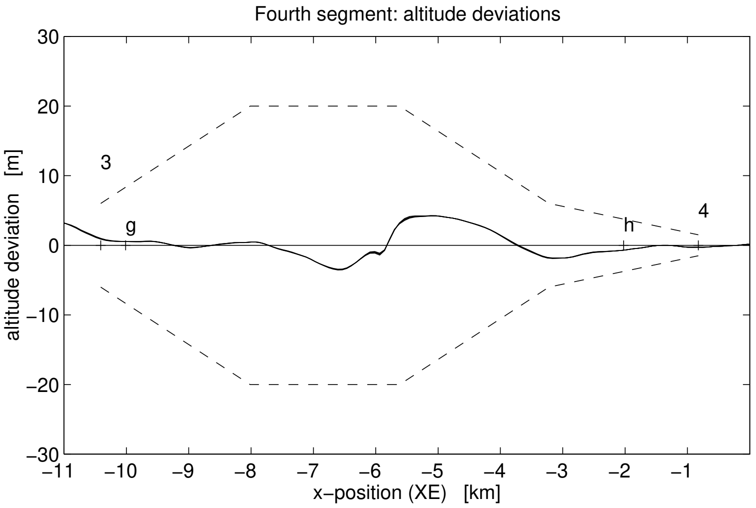

Fig.7.8 Segment IV: vertical deviations from the desired glide-slope

as a value greater than one of the corresponding indicator. Also, in segment IV, in order to comply with the vertical wind-shear disturbances, the passengers comfort is decreased (indicator > 1). Apart from these values greater than one of the comfort indicator, all other indicators show a good achievement of the design challenge requirements.

	Segment I	Segment II	Segment III	Segment IV	Total
Performance	0.5153	0.2792	0.1943	0.1138	0.2756
Robustness	0.0797	0.0675	0.0882	0.0601	0.0739
Comfort	0.6027	1.7584	0.6723	1.2348	1.0671
Safety	0.0081	0.0228	0.0100	0.0250	0.0165
Power	0.0055	0.0077	0.0151	0.0295	0.0145

Table 7.1 Numerical results of the evaluation procedure

8 Conclusions and lessons learned

In this report the aim has been to provide the reader with information about applying MBPC to aircraft control. The design method is illustrated by designing an autopilot for the RCAM used in the Group for Aeronautical Research and Technology in Europe (GARTEUR) design challenge [2]. To enable comparisons with other GARTEUR designs a standard evaluation over a *Frankfurt descent procedure* was performed [3] which tested the controller in conditions of mismodeling, gust disturbances and an engine failure.
A design environment was developed, which was intended to be a useful tool for MBPC controller development. Despite the non-conventional structure of MBPC, the resulting controller has standard interfaces to the evaluation software, and at a high level is " plug-compatible" with a conventional controller.

Evaluating and discussing the design challenge results
A principal reason for developing this design was to demonstrate that MBPC can be applied to a realistic complex benchmark problem and to demonstrate the limitations of this technique.
The design of the automatic pilot, done for the final approach of an experimental fictitious aircraft (RCAM) is robust with respect to variation of several model parameters, time delays, nonlinearities and engine failures. As regards robustness analysis, in Section 7.2 we have shown that the controller behaviour is generally satisfactory with significant model uncertainties. This exercise also had the goal of evaluating and presenting the method's limitations. Ride quality criteria such as maximum vertical acceleration, maximum lateral acceleration and damping were computed after the evaluation mission was completed, and are presented in table 7.1. Apart from two values greater than one of the comfort indicator, all other indicators from table 7.1 show good achievement of the design challenge requirements.
We want to stress again the issue of robustness addressed during the design. The main achievement is that we use a MBPC controller based on a single linear internal model – a state space realisation that does not contain actuators models. The behaviour of the controlled aircraft was proved to be good across the whole flight envelope. Moreover, the implementation of the MBPC controller as a Stability Augmentation System (SAS) proved to be satisfactory in terms of performance achieved during various manoeuvres. Disturbance rejection of wind-shear and gust is good as well as tracking during engine failure or constant wind shear.
Another problem is that a constrained optimisation problem must be solved on-line, and therefore the computational complexity of implementing the controller is high. The main implementation difficulty is in reducing the computation time sufficiently to allow real-time operation. The latter problem is probably not insuperable, because progress can be expected both in the efficiency of solution algorithms for MBPC [8], and in the power of the hardware on which they run.

Lessons learned

The main difficulty in designing MBPC is in the tuning of the many parameters available in the algorithm. But we found that with experience developed tuning procedures, based partly on theoretical results, which were partly systematic.
It was possible to obtain a satisfactory controller despite a very simple model used as an internal model for the MBPC. But, some aspects of its performance, particularly robustness, were achieved in a trial-and-error manner, by post-design testing. In order to move towards more systematic design, from the robustness point of view, it is necessary to use a multi-model approach to ensure robustness against large perturbations (eg. engine failures).

General remarks

Constrained Model Based Predictive Control may not offer any advantages over more conventional control algorithms for routine flight control applications, apart from the constraint handling. As mentioned at the beginning of this Report, however, we believe that it has good potential for higher-level control functions, such as on-board flight management, or reconfiguration of controllers in the event of damage to the aircraft structure or equipment.
We are currently extending our research to the combined use of $\mathcal{H}_\infty$ loop-shaping and $MBPC$ as a method of designing automatic pilots for civil aircraft. An $\mathcal{H}_\infty$ loop-shaping controller in the inner loop will provide the stability augmentation and guidance functions; an $MBPC$ controller in the outer loop controller will act as a flight manager and overall supervisor [9].

References

[1] Flight Mechanics Action Group 08. Communication handbook, version 2. In TP-088-5, editor, *GARTEUR*. FM(AG08), 1996.

[2] Flight Mechanics Action Group 08. Robust flight control design challenge problem formulation and manual: the research civil aircraft model (rcam), version 2. In TP-088-3, editor, *GARTEUR*. FM(AG08), 1996.

[3] R. Brockhaus. *Flugregelung*. Springer Verlag, Berlin, 1994.

[4] H.W. Chiou and E. Zafiriou. Frequency domain design of robustly stable constrained model predictive controllers. In *American Control Conference*, volume June, pages 2852–2856. Baltimore, Maryland, 1994.

[5] D.W Clarke and C. Mohtadi. Properties of generalized predictive control. *Automatica*, 25(6):859–875, 6 1989.

[6] G.E. Garcia D.M. Prett and C.R. Cutler. The dynamic matrix control method. *US Patent 4349869*, 9 1982.

[7] C. Mohtadi D.W Clarke and P.S. Tuffs. Generalized predictive control i and ii. *Automatica*, 23(2):137–160, 1987.

[8] Systolic Architectures for iterative LQ Optimisation. L.chisci and g. zappa. *Automatica*, 27:799–810, 1991.

[9] K. Glover G. Papageorgiou, M. Huzmezan and J. Maciejowski. Combined MBPC/H-inf autopilot for a civil aircraft. *submitted to ACC*, 1997.

[10] S.A. Heise and J.M. Maciejowski. Stability constrained MBPC using a internal model control structure. In D. Clarke, editor, *Advances in Model-Based Predictive Control*, pages 230–244. Oxford University Press, 1993.

[11] J.L. Testud J.A. Richalet, A. Rault and J. Papon. Model predictive heuristic control: Aplications to an industrial process. *Automatica*, 14:413–428, 1978.

[12] D. McFarlane and K. Glover. A loop shaping design procedure using h_∞ synthesis. *IEEE Transactions on Automatic Control*, 37(6):759–769, June 1992.

[13] D. McFarlane and K.Glover. An h_∞ design procedure using robust stabilization of normalized coprime factors. In *IEEE Proceedings of the* 27^{th} *Conference on Decision and Control*, volume 2, pages 1343–1348. Austin, Texas, 1988.

[14] D.C. McFarlane and K.Glover. *Robust Controller Design Using Normalized Coprime Factor Plant Descriptions*. Springer-Verlag, first edition, 1989.

[15] R.Hyde and K.Glover. Taking h_∞ control into flight. In *IEEE Proceedings of the 32^{nd} Conference on Decision and Control*, volume 2, pages 1458–1463. San Antonio, Texas, 1993.

[16] A.R.M. Soeterboek. *Predictive Control - A unified approach.* Prentice Hall, New York, first edition, 1992.

[17] J.M. Deinert W. Kossman and S. Park. Model-based control of a partial burn fluid cathalytic cracking unit. *IEE Computing and Control*, 6:17–21, 1995.

A The software used

In this Section we include only the heart of the MBPC algorithms namely, the optimiser. All matrices involved in the algorithm are computed off line.

```
function [sys,x0] = optimiser(t, x, u, flag, ll, mm, nn, mu_sys,ns_sys,
po_sys, NNu, NN2, Uo, Xo, Yo, X_pred, A_new, B_new, D_new, E_new, Ts)

% S-function that solves the predictive control problem
% author: Mihai Huzmezan, University of Cambridge, Control Group, 25 March 1996

% Sample and offset times
offset = 0;
ts = Ts;
if abs(flag) == 1 %                    return derivatives
  sys = [];
elseif abs(flag) == 2 %                return discrete states in sys
  sys = [];
elseif flag ==3 %                      return outputs
  % Is it a sample hit (within a tolerance of 1e-8) ?
  if abs(round((t-offset)/ts)-(t-offset)/ts)<1e-8
    % Load current plant inputs, states and outputs
    time = u(1);
    U = u(2:(mu_sys+1));
    Y = u((mu_sys+2):(mu_sys+po_sys+1));
    X_pred1 = u((mu_sys+po_sys+2):(mu_sys+ns_sys+po_sys+1));
    comm = u((mu_sys+ns_sys+po_sys+2):(mu_sys+ns_sys+po_sys+po_sys+1));
    if t == 0
      % Initial step at t = 0
      J = [];
      U = Uo;
      Y = Yo;
      X_pred1 = X_pred;
      comm = Yo;
    end
    % Reference trajectory generator; S = reference to be followed over the prediction horizon
    aux = Y;
    S = Y;
    step = (comm-Y)/(NN2-2);
    for k = 1:NN2
      S = [S;aux];
      aux = aux+step;
    end
    S = S(1:(po_sys*NN2));
    % QP initialization
    ccc = [X_pred1' Y' S']*B_new;
    bbb = E_new*[U;X_pred1;Y;ll;mm;nn];
    AAA = D_new;
    QQQ = A_new;
    % The QP solver (see Optimization Toolbox)
    Delta_U_0 = qp(QQQ,ccc',AAA,bbb);
    Delta_U = Delta_U_0(1:mu_sys);
    sys = Delta_U;
    if abs(Delta_U) < 1e-10*ones(mu_sys,1)
      sys = zeros(1,mu_sys);
    end
  else
    sys = zeros(1,mu_sys);
  end
elseif flag == 4 % retun next sample hit
  % ns stores the number of samples
  ns = (t-offset)/ts;
  % this is the time of next sample hit
  sys = offset+(1+floor(ns+1e-13*(1+ns)))*ts;
elseif flag == 0, % return initial conditions and size informations
  sys = zeros(6,1);
  sys(1) = 0;  % number of continous state, 0 - not a dynamic system
  sys(2) = 0;  % number discrete state, 0 - not a dynamic system
  sys(3) = 3;  % number of system outputs
  sys(4) = 17; % number of system inputs
  sys(5) = 0;  % no roots
  sys(6) = 0;  % no direct feedthrough
  x0 = [];
else
  sys = [];
end
```

The main software components are located on the FTP site opened at University of Cambridge with the following address: ftp.eng.cam.ac.uk.

B The designer's background

The designer experience in flight mechanics/control was accumulated during five years of study for an MSc degree at The University "Politechnica" Bucharest - Aerospace Faculty between 1988-1993.

The experience with the application of the described method, MBPC control, has been gained while the designer has been studying for a PhD degree at The University of Cambridge since January 1995.

Much of the learning time was spent in producing a simulation framework suitable for a general problem in parallel with understanding the tuning mechanisms of MBPC. When these steps were accomplished we had a gross iteration to tune the MBPC inner controller for each of the channels followed by the design of outer conventional controllers. Several iterations were made in order to achieve the present tuning, which resulted in a better understanding of the technique.